TETRONIC CAPPED MESOPOROUS SILICA NANOPARTICLES FOR DRUG DELIVERY

by

Sezi Yiğit

B.S., Chemical Engineering, Middle East Technical University, 2016

Submitted to the Institute for Graduate Studies in
Science and Engineering in partial fulfilment of
the requirements for the degree of
Master of Science

Graduate Program in Chemical Engineering

Boğaziçi University

2019

ACKNOWLEDGEMENTS

Firstly, I would like to express my sincere thanks to my advisor Asst. Prof. Nazar İleri Ercan for her outstanding guidance, encouragement and contribution during my studies. I think I was so fortunate that I had the opportunity to work with her and I will always remember her politeness and patience toward me. She has been a role model for me and it was a great honor for me to work with her.

I would like to thank my thesis committee members; Prof. Kutlu Ülgen and Assoc. Prof. Seda Kızılel for devoting their valuable time for my thesis defense.

I wish to express my gratitude to Özlem Özbek, Feyza Kevser Öner and Selin Taşkın for their guidance and valuable help throughout my work.

Very special thanks goes to my friends Özüm Özelge, Eylül Balcılar, Numan Su, Can Baycan, Eylül Ecem Tekin and Aslı Yılmaz for their emotional support and motivation throughout my master education. This thesis would not have been possible without their everlasting support.

Last but not least, my dearest thank is for my beloved mother, my father, and İsmail Üstün for their endless love and support along the way. They always believed in me throughout my life.

Finally, financial support provided from BAP (SUP:17A05SUP2) is gratefully acknowledged.

ABSTRACT

TETRONIC CAPPED MESOPOROUS SILICA NANOPARTICLES FOR DRUG DELIVERY

In this study, Tetronic capped mesoporous silica nanoparticles are synthesized and characterized. The efficiency of the gating mechanism is investigated for drug delivery purposes. For this reason, mesoporous silica nanoparticles (MSNs) are produced and coated with Tetronic as gates. Pluronic is also used as an alternative copolymer to compare the results with Tetronic. Two approaches are used to gate the MSNs, which are the physical attachment method and the covalent bonding method. For the physical attachment method, hydrophobic MSNs (hMSNs), in other words, octyl modified MSNs are produced. By making use of the hydrophobic/hydrophilic nature of the copolymers, physical attraction between PPO (hydrophobic) part of the copolymers and the hydrophobic surface of hMSN is achieved. In order to investigate the gating mechanism, efficiency of the physical attachment method, hMSNs are loaded with curcumin before gating with Tetronics. After coating the surface with the copolymer, release experiments at different temperature and pH values are performed and analyzed with UV-Vis spectrophotometry. The highest release rate is obtained at 37℃ and pH 4.8 for Tetronic and at 43℃ and pH 7.4 for Pluronic. In the chemical method, after amination and carboxylation of both MSNs and copolymers, covalent bonding is achieved between MSNs and copolymers through the click chemistry. The success of carboxylation and amination of the materials is confirmed with FTIR spectoscopy. For carboxyl functionalized MSNs and aminated Tetronics / Pluronics, release experiments are conducted using arginine. The highest release rate is achieved at 37℃ and pH 4.8 for MSNCOOH-T1107NH_2 and the minimum release data is obtained at 37℃ and pH 4.8 for MSNCOOH-F127NH_2. Finally, in order to investigate the toxicity of nanoparticles, *Saccharomyces cerevisiae* is used as a model cell and CFU analysis is performed. Physical attachment method is observed to be more toxic compared to the chemical attachment method.

ÖZET

İLAÇ DAĞITIMINDA TETRONİK KAPLI MEZOGÖZENEKLİ SİLİKA NANOPARTİKÜLLER

Bu çalışmada, Tetronic kaplı mezo gözenekli silika nanopartiküller sentezlenmekte ve karakterize edilmektedir. Ayrıca ilaç salınımının performansını araştırmak amacıyla kapı sistemi kurulmuştur. Bu amaçla, çeşitli mezo gözenekli silika nanoparçacıkları (MSN) üretilmiş ve Tetronic ile kaplanmıştır. Pluronic, sonuçları Tetronic ile karşılaştırmak üzere alternatif bir kopolimer olarak kullanılmıştır. MSN üzerinde kapı sistemi oluşturmak için fiziksel bağlama yöntemi ve kovalent bağlama yöntemi izlenmiştir. Fiziksel bağlama yöntemi için, hidrofobik MSN'ler (hMSN'ler), başka bir deyişle oktil olarak değiştirilmiş MSN'ler üretilmiştir. Kopolimerlerin hidrofobik / hidrofilik özelliği kullanılarak, kopolimerlerin PPO (hidrofobik) kısmı ile hMSN'nin hidrofobik yüzeyi arasında fiziksel çekim sağlanmıştır. Fiziksel bağlama yönteminde kapı mekanizması etkinliğini anlamak için, kapı mekanizması oluşturulmadan önce hMSN'lere zerdeçal yüklenmiştir. Yüzeyin kopolimer ile kaplanmasından sonra, farklı sıcaklık ve pH değerlerinde salım deneyleri UV-Vis spektroskopisi ile gerçekleştirilmiştir. En yüksek salım oranı Tetronic için 37°C'de ve pH 4.8'de ve Pluronic için 43°C'de ve pH 7.4'te gözlenmiştir. İkinci yöntemde, hem MSN'lerin hem de kopolimerlerin aminasyon ve karboksilasyonundan sonra, klik kimyası kullanılarak kovalent bağlama, MSN'ler ve kopolimerler arasında yapılmıştır. Karboksilasyonun başarısı ve malzemelerin aminasyon işlemi FTIR spektoskopisi ile doğrulanmıştır. Karboksil uçlu MSN'ler ve amin uçlu Tetronic / Pluronic için, kargo molekülü olarak arginin kullanılarak salım deneyleri gerçekleştirilmiştir. MSNCOOH-T1107NH_2 için 37°C ve pH 4.8'de en yüksek salım verilerinin olduğu ve MSNCOOH-F127NH_2 için minimum salım verilerinin 37 °C ve pH 4.8'de olduğu gözlenmiştir. Ayrıca, nanopartiküllerin biyouyumluluğunu araştırmak için model maya hücreleri ile CFU analizi yapılmıştır ve fiziksel bağlama yönteminin kimyasal bağlama yöntemine kıyasla daha toksik olduğu gözlemlenmiştir.

TABLE OF CONTENTS

LIST OF FIGURES

LIST OF TABLES

LIST OF SYMBOLS

A	Absorbance (no units)
c	Concentration (M)
D	Diffusion coefficient
d_H	Hydrodynamic diameter
k	Boltzmann's constant
L	Path Length (cm)
T	Absolute temperature
ε	Extinction coefficient (specific to each substance) (cm^{-1})
η	Viscosity

LIST OF ACRONYMS/ABBREVIATIONS

F127-CDI	CDI-activated Pluronic F127
F127-NH_2	Amino terminated Pluronic F127
F127NH_2-MSNCOOH	Crosslinking of carboxylated MSN and aminated Pluronic F127
hMSN	Hydrophobic Mesoporous Silica Nanoparticles
MSN	Mesoporous Silica Nanoparticles
MSN-COOH	Carboxylic acid functionalized Mesoporous Silica Nanoparticles
MSN-NH_2	Amino functionalized Mesoporous Silica Nanoparticles
T1107-CDI	CDI-activated Tetronic T1107
T1107-COOH	Carboxylated T1107
T1107COOH-MSNNH_2	Crosslinking of aminated MSN and carboxylated Tetronic T1107
T1107-NH_2	Amino terminated Tetronic 1107
T1107NH_2-MSNCOOH	Crosslinking of carboxylated MSN and aminated Tetronic T1107

1. INTRODUCTION

Cancer is one of the leading causes of morbidity and mortality worldwide, with approximately 14 million new cases in 2012 [1]. Chemotherapy is the primary treatment for cancer; however, its success rate is not high as expected [2,3]. The primary reason for the failure of chemotherapy is the poor accessibility of antineoplastic agents to the tumor cells, requiring higher doses, and the nonselective nature of these agents causing severe toxicity [3]. Therefore, nanocarrier mediated drug delivery has emerged as an alternative approach to reduce the side effects and improve the performance of anticancer drugs in cancer therapy. Among the nanocarriers, mesoporous silica nanoparticles (MSNs) have attracted increasing attention as novel nanocarriers for on-demand drug release, and have been variously synthesized for cancer imaging, and simultaneous diagnosis and therapy over the past decades [2,4].

Mesoporous silica nanoparticles (MSNs), are solid particles, which are composed of porous structures with empty channels that enable them to hold/encapsulate the bioactive molecules in comparably large amounts. MSNs' high surface area and pore volume, unique physicochemical and biochemical stability, together with a number of other convenient structural features, such as uniform and tunable pore size, effortless surface functionalization ability, make them valuable inorganic drug carriers and theranostic agents for biological applications [2,5]. However, bare MSNs can not meet the expectations of zero premature release, cell and tissue specifity, and targeting ability, to release the encapsuled materials with a desired rate and to achieve an adequate local concentration and biocompatibility. The bare silica surface is covered with negatively charged silanol groups, which can interact electrostatically with the positively charged tetraalkylammonium parts of the cell membrane and cause cytotoxicity by membranolysis or obstruction of cellular respiration [5]. Additionally, bare silica nanoparticles may cause death and organ failure by the sudden collection of the silica particles in the biological media. For example, they cause mechanical blockage in the capillary vessels of vital organs [5]. The surface charges of bare nanosilica particles result in their

recognition and capture by the reticuloendotelial system (RES) and hence bare MSNs can be cleared through RES within a short time after being injected into the blood vessel [6].

The success of the target-specific drug delivery system approach relies on the plausibility of designing a biocompatible carrier that promises transportation of highly loaded drug molecules without any leakage before the drug reaches the targeted cell. At this point, in order to keep the drug inside the pores of MSNs and accomplish stimuli-responsive drug release, the outer surface of the MSN is often functionalized with different types of gating entities, such as dendrimers, nanoparticles, quantum dots, proteins, antibodies, and natural or synthetic polymer coatings which can alter their structure upon environmental changes [4]. This modification also helps to increase the biocompatibility of MSNs, minimize their recognition by RES and increase the blood circularion times.

Amphiphilic copolymers are a group of polymers that can provide the gating mechanism. They contain both a hydrophilic and a hydrophobic block tethered to each other and they aggregate automatically in water to build supramolecular structures. The hydrophobic part of amphiphilic copolymers makes a proper host for poorly-soluble drugs, while the hydrophilic part aids in physically stabilizing the molecule as it aggregates in the aqueous environment. Regarding the blood circulation time and the desired drug release rate, the structure/architecture of the copolymer can be tuned in order to meet the theraupatic demands. Among various types of copolymers used for gating purposes, pluronics and tetronics are popular as they can surpass the limitations. Pluronics consist of two hydrophilic polyethylene oxide (PEO) blocks connected to a central hydrophobic polypropylene oxide (PPO) block or vice versa [7]. On the other hand, the X-shaped counterpart of pluronics, known as tetronics or poloxamines, consist of ethylenediamine central group bonded to four chains of PPO-PEO blocks. PEO blocks in these copolymers partially limit the adsorption of proteins to the polymer surface and hence prevent the recognition of the polymer by macrophages and extend its circulation in the bloodstream [7]. Moreover, PEO/PPO mass ratio determines hydrophilic-lipophilic balance (HLB). HLB plays a critical role in determining the biological activity of the polymer. For example, it has been shown that pluronics can enhance gene transcription [8], increase the sensitivity of multidrug resistant cells in vitro and in vivo [9], diminish biofilm formation [10], seal damaged

cell membranes and restore their integrity [11,12], or facilitate the passage of molecules across the lipid membranes and increase the membrane permeability [13,14], all depending on HLB and molecular weight of the polymer.

Pluronics and tetronics are stimuli-responsive copolymers, therefore they can release the cargo in precise locations at rates controlled by an external activator. That is, the release of the encapsulated drug can be controlled by self-regulation of the polymeric gate in response to the changes in the microenvironmental conditions. The reasons, i.e. signs or stimuli, that trigger the structural changes in the copolymer, can be classified in three groups: physical stimuli (temperature,ultrasounds,light,mechanical stress), chemical stimuli (pH and ionic strength) and biological stimuli (enzymes and biomolecules) [15]. Among these stimuli, pH and/or temperature(T) responsiveness are the most studied properties due to the differences in pH/T conditions between cancer cells and healthy cells [15]. In this sense, thermoresponsive pluronics have been proven to be efficacious candidates in medical applications. Four armed poloxamines containing an ethylenediamine group, on the other hand, have greater chemical versatility and dual pH and temperature responsive behaviour compared to pluronics [16]. Therefore, tetronics can offer unique features as gating agents of MSNs in targeted drug delivery.

2. THEORY

According to Slowing *et al.*, (2008), the failure of conventional method such as chemotherapy and cytotoxic drugs is due to lack of target specifity feature of current anticancer drugs. At this point, target-specific drug delivery system (DDS) is introduced as a new and alternative method which can store desired amount of drug molecules until the targeted cells and tissues. Certainly, the success of this system is linked with the ability to design a biocompatible carrier which has high capacity of drug loading without any premature release before reaching the target destination. In order to construct an efficient drug delivery system (DDS), some prerequisites are need to be integrated.

- Biocompatible nanocarrier
- High loading/encapsulation capacity for drug molecule
- Compatible hydrophobic/hydrophilic nature between particle and drug structure
- Zero premature release (no leakage)
- Cell type or tissue specificity
- Ability to route the target (recognition of target cell)
- Controlled release of drug molecules with desired rate to provide an effective local concentration

Several biodegradable materials, such as polymeric nanoparticles, dendrimers, and liposomes meet with these expectations. These “smart” drug delivery systems can controllably release cancer/pharmaceutical drugs in aqueous media through degradation of the carrier triggered by various conditions. (pH, temperature etc.)

Although several exciting DDS systems have been accomplished with this approach, zero premature release of drugs are very struggling with these structurally unstable “soft” materials. In many cases, once the system was introduced into the aqueous solution, encapsulated drug molecules would start leaking out the biodegradable nanocarrier [17]. As a relatively recent

method, nanoparticles are started to participate in cancer therapy research in the few last decades. These materials have some unique advantages because they can provide a prolonged release and effective drug delivery [18].

Over the three decades of research on MSNs, as nanocarriers for drug delivery applications, has revealed that MSNs with their sophisticated mesoporous architecture has specific advantages which is proper for clinical applications. First of all, MSNs can be tailored in terms of shape, size, surface chemistry and mesoporous or hollow structures. This property of MSNs is very beneficial because the drug delivery system requires extraordinarily high drug loading capacity and stimuli-responsive drug release profile. Secondly, MSNs have comparatively high biocompatibility properties both in vivo and in vitro, and they can be discharged from the body over time. Thirdly, for simultaneous bioimaging and drug delivery for nanotheranostic applications, the easiness of multifunctionalization with magnetic, fluorescent, and photothermal entities is very useful. Moreover, to maintain future industrial production and clinical translocation, synthesis of MSNs has unique advantages over other methods because it is flexible, scalable and cost-effective. Overall, MSNs have been shown to hold many desired properties for drug delivery applications, but these nanocarriers are still developing and many research has been going on in this field [6].

The effects of geometry, porosity, surface chrage, and size of MSNs on cellular toxicity and hemolytic activity are among the research topics. For example, Yu *et al*., (2011) have studied the effects of geometry, porosity, and surface charge using nonporous and mesoporous silica nanospheres and demonstrated that the toxicity of silica is cell-type dependent and that surface charge and pore size govern cellular toxicity. In the same study, the hemolytic activity was demonstrated to be porosity- and geometry-dependent for bare silica and surface charge dependent for amine-functionalized silica nanoparticles. Ferenc *et al*., (2016) have recently studied different SBA-15 type nanoparticles sharing similar morphology, silanol density and siloxane condensation degree but different surface groups (amine, thiol and carboxlic groups) and demonstrated that irrespective of functional groups silica interacts with human serum albumin and results in suppresion of hemolysis. Kim *et al*., (2015), have studied the size and

dose effects of silica nanoparticles with diameters between 20 nm -200 nm and found that the cytotoxicity of silica nanoparticles depends highly on cell type apart from the size and dose.

Morphology changes in MSNs based on diffrences in fabrication methods is another research topic in this field. Yıldırım and Bayındır, (2015) have reported a method based on selective dissolution of porous cores of solid silica shell/porous silica core nanoparticles using phosphate buffered saline at 65 °C. Synthesized hollow nanoparticles had both small and large mesopores making the nanoparticle ideal for encapsulating a wide range of molecules. Tu *et al.*, (2016) have synthized large pore MSNs using a double surfactant system consisting high molecular weight pluronics and revealed that these structures are ideal for encapsulating proteins and enzymes. Similarly, Yu *et al.*, (2017) have synthesized MSNs with expanded pore sizes by treating the nanoparticles hydrothermally and demonstrated that these nanoparticles can be used to deliver higher molecular weight molecules such as proteins.

Most of the studies on MSNs in drug delivery applications, however, have been focused on the surface functionalization of MSNs. To date, MSNs have been coated/encapsulated with different materials including peptides [24], enzymes [25], metal ions [26], liposomes [27], several polymers i.e. polydopamicine (PDA), polyvinyl pyrrolidone (PVP), polyvinyl alcohol (PVA), polyacrylamide (Pam) [28], and some natural polysaccharides i.e. Dextran (Dex), polysialic acid (PSA), hyaluronic acid (HA), chitosan (CH) [24] for gating purposes. Yet, the use of pluronics in surface modification of MSNs has only very recetly started to capture attention.

Yildirim *et al.*, (2013) have studied a straightforward self-assembly method by using octyl modified hydrophobic MSNs and an amphiphilic block copolymer (F127) and demonstrated that, F127-OMSN yields in good stability and great dispersibility in both water and PBS (phosphate buffered saline, pH = 7.4) at high concentrations of salty media. Moreover, MSNs capped with uncharged F127 molecules have been completely prevented from the hemolytic activity even at high particle concentration by intercepting the electrostatic interaction of silanol groups with the RBC membrane, whereas bare MSNs have shown remarkable hemolytic activities. However, both MSN and F127-OMSN have been demonstrated to be highly

compatible with MCF-7 (human breast cancer cell line) cells after incubation times of 24 or 48 h.

Xu *et al*., (2015) developed and manufactured a nanocarrier by collaborating mesoporous silica nanoparticles and F127 micelles, aiming to obtain a proper method for the design of multifunctional stimuli-responsive drug delivery and self-fluorescent imaging systems. In this design, CF127 (curcumin-F127), F127 micelle loaded with anticancer drug (curcumin), was utilized as a gating agent on mesoporous silica nanoparticles. pH-sensitive Schiff base resulted in drug release from the gating micelles under acidic condition, whereas the drug release was blocked under neutral conditions. CF127 micelles showed good anti-photobleaching property, allowing them to be used in noninvasive in vivo tracking of the delivery of therapeutic agents. In recent years, several polymeric hydrogel nanoparticulate designs based on both natural and synthetic polymers have been prepared and characterized for drug delivery purposes [29].

Therefore, incorporation of pluronics and tetronics into polymeric nanoparticles and their use as micellar structures in drug delivery have been studied in a wider manner. For example, Hu *et al*., (2015) have developed a thermo responsive pluronic in situ forming hydrogel for co-delivery of paclitaxel and lapatinib and demonstrated that the system had higher efficiacy on survival rate for tumor bearing mice with lower levels of toxicity. Additionally, Dehghankelishadi *et al*., (2016) have developed a pluronic F127/L61 micellar system which is used for delivery of doxorubicin for treatment of Adenocarcinoma. The system, also, increased the survival rate of tumor bearing mice significantly and decreased the levels of toxicity. The system has successfully completed phase 1 and 2 only in clinical studies. Ribeiro *et al*., (2012) have studied polymeric micelles of single and mixed poloxamines (tetronics) regarding their ability to host the antiglaucoma agent ethoxzolamide (ETOX) for topical ocular glaucoma therapy, and showed that co-micellization of poloxamines with different hydrophilicity gives physically more stable systems that maintain more efficient ETOX release compared to micelles of single components. Moreover, Greenebaum *et al*., (2004) have studied the protection of skeletal muscle cells after exposure to irradiation using P188 poloxamers and showed that there has been greater survival in treated cells.

2.1. Synthesis of Mesoporous Silica Nanoparticles

A base-catalyzed sol–gel process are performed to produce silica nanoparticles with proper sizes for biomedical applications. Organosilane precursors (TMOS, TEOS, etc.) are employed for the sol–gel process which are hydrolysis and condensation reactions.

$$\textit{Hydrolysis: } OH^- + Si(OR)_4 \rightarrow Si(OR)_3OH + RO^- \quad (2.1)$$

$$\textit{Condensation: } SiO^- + Si(OH)_4 \rightarrow Si - O - Si + OH^- \quad (2.2)$$

These two reactions provide the formation of sol phase. Then small colloidal particles inside the sol condense into gel phase. Stöber process has been broadly applied for the synthesis of monodispersed silica nanoparticles between 50 and 2000 nm size, using the ammonia-catalyzed hydrolysis of tetraethylorthosilicate (TEOS) in a water-alcohol solution. By using cationic surfactant as templating agent which is formed by micelles, the silicate materials can be directed to condense around the cationic surface template into ordered silica structures [19].

2.2. Characterization Methods

2.2.1. Dynamic Light Scattering (DLS)

Dynamic Light Scattering is a technique to understand the particle size of a sample. DLS is also known as Photon Correlation Spectroscopy or Quasi-Elastic Light Scattering. So, three different names for the same non-invasive technique. In other words, sample is placed in tube then laser directed into that sample, however the sample is not affected at all by the laser. When sample is taken out of the instrument, it is exactly in the same state with before. This technique is capable of measuring the size of particles and molecules in suspension. Important part for this technique is Brownian motion which is a random movement. So, these particles and molecules are moving around randomly because they are constantly being bombarded by the solvent molecules around them and dynamic light scattering measures the speed at which these particles undergo this Brownian motion. Small particles diffuse rapidly, and the larger the particle, slower

diffusion will be. The velocity of this Brownian motion is called the translational diffusion coefficient (D). Moreover, diffusion coefficients are converted into size through the Stokes Einstein equation (2.3). Also, temperature should be known since viscosity of the liquid is related with temperature [33]. The translational diffusion coefficient can be converted into a particle size/hydrodynamic size using the Stokes-Einstein equation.

$$d_H = \frac{kT}{3\pi\eta D} \tag{2.3}$$

Where,

d_H : Hydrodynamic diameter

k : Boltzmann's constant

T : Absolute temperature

η : Viscosity

D : Diffusion coefficient

Hydrodynamic diameter is defined as the diameter of a hard sphere that diffuses at the same speed as the particle or molecule being measured. And it depends on several concepts like ionic strength, surface structure, shape. Ionic strength influences inversely the thickness of the cloud of ions that exists around the particles in other words Debye length. Surface structure is also an important feature which effects hydrodynamic diameter. If there are nodes or polymer layer on the surface, in this way molecules are sitting out into the medium which influences the diffusion speed.

All DLS samples were prepared with deionized water, and concentration was different for different types of samples. In some cases, filtration was used to prevent inconsistent results. The brand of the instruments is Brookhaven Instruments 90Plus Particle Size/Zeta analyzer.

2.2.2. Fourier Transformed Infrared (FTIR)

Fourier Transformed Infrared (FTIR) is a sensitive tool to understand chemical identification. Each chemical bond and molecule gives specific and unique frequency or spectral fingerprint, in this way, a change in a chemical structure of a sample can be detected. Basically, infrared light passes through the material and depending on its energy, this can trigger the vibration of specific molecular bonds which is called absorption. There are different kinds of vibrations which are symmetric stretching vibration, anti-symmetric strecthing vibration and deformation vibration.

In FTIR analysis, infrared light is directed to the sample. While some light is reflected, the sample absorbs specific amounts of the light passes through sample. The remaining light which carries molecular information of the sample is transmitted and collected by detector to produce electronic signal. As illustrated in Figure 2.1, during the measurement IR-beam enters the interferometer and is directed at a beamsplitter.

The beam is then split, and directed at a fixed and moving mirror respectively. Then the light travels back to the beamsplitter where the beam is recombined causing interference and finally directed at the sample material. The spectral information of all wavelengths is acquired simultaneously. Then these signals are transformed into graphs as shown in Figure 2.1.

There are two modes for FTIR analysis which are ATR and KBr mode. ATR mode is usually used for surface analysis without and extra materials or holder. However, in KBr mode there are two KBr discs to compress the sample under vacuum.

In this research, KBr method was chosen because samples might hold moisture without vacuum. The brand name of the instrument is Vertex 80V.

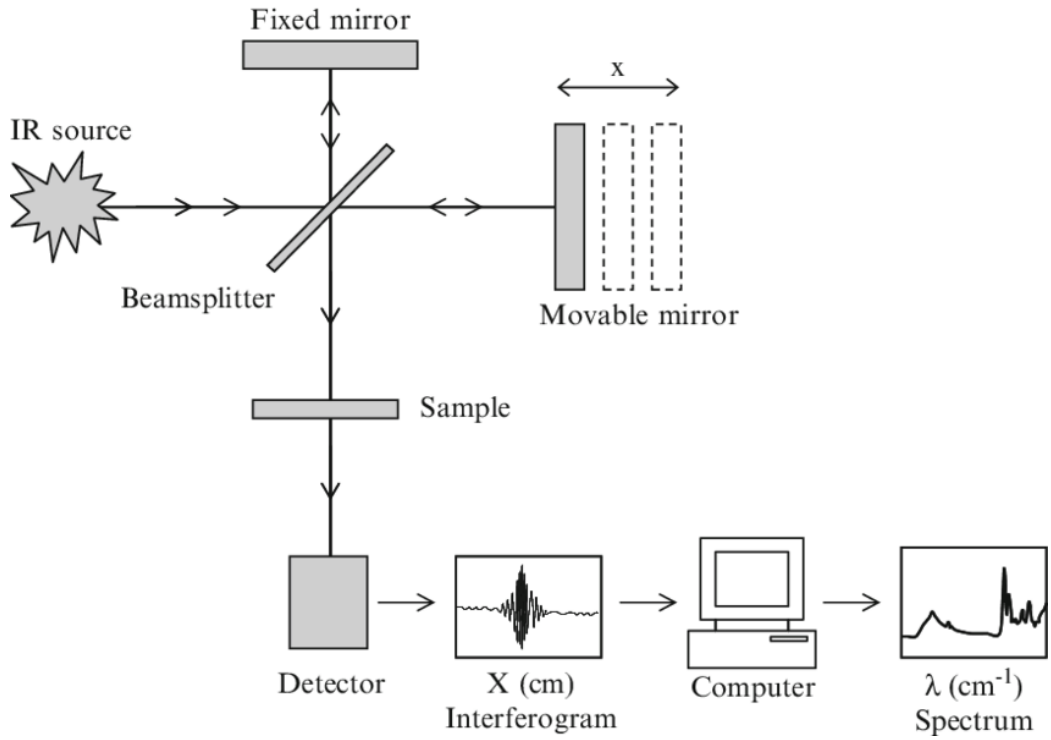

Figure 2.1. Schematic Diagram of FTIR [34].

2.2.3. Scanning Electron Microscopy (STEM/SEM)

Scanning Electron Microscope (SEM) and Scanning Transmission Electron Microscope (STEM) are techniques of electron microscope to attain images of sample surface by scanning the surface with focused beam electrons. Beamed electrons either get absorbed, reflected or get through the sample. Reflected electrons are in the form of backscattered electrons, secondary electrons, X-rays and also some auger electrons but only the secondary electrons detected by the detector for these imaging techniques. There are two modes of a microscope which are scanning mode (SEM) and transmission mode (STEM).

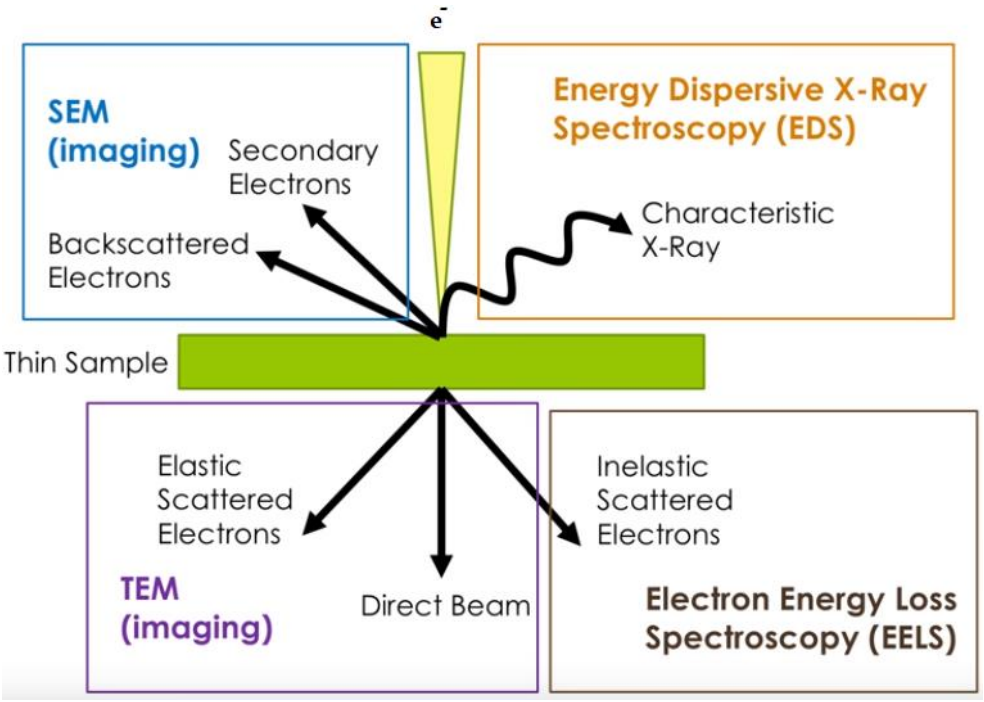

Figure 2.2. Schematic of electron interactions.

2.2.3.1. Scanning Electron Microscopy (SEM). In a typical SEM technology, electron source is focused into a beam which has approximately final spot size of 5nm, having energy ranging from a few hundred electron volts to 50 keV. Electron beam scans object in raster scan patterns which means that object is scanned side by side therefore 3D images are attained by collecting the emmited electrons [35].

2.2.3.2. Scanning Transmission Electron Microscopy (STEM). Scanning transmission electron microscope (STEM) is like a combination of the scanning electron microscope (SEM) and transmission electron microscope (TEM). SEM imaging is useful for surface inspection and TEM is like microscopes allow for a closer look at the material and identify material properties down to nano scale. In STEM, all these features are possible, allowing for a correlation between surface information and bulk information. By STEM, liquid samples can also be analyzed. The brand of the instrument is EDAX-Energy Dispersive X-Ray Analysis Unit.

2.2.4. Ultraviolet- Visible Spectroscopy (UV-VIS)

Ultraviolet- Visible Spectroscopy (UV-VIS) is a method to detemine concentration of an analyte in the solution. UV-VIS spectrophotometer performs optical spectroscopy which is a method that investigates how light interacts with matter in the ultraviolet and the visible range of light as shown in Figure 2.3.

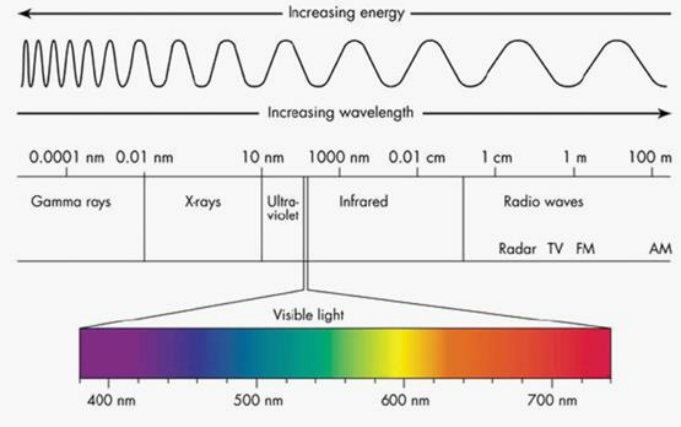

Figure 2.3. UV-Vis Light Spectrum [36].

There is a linear relationship between how much light is absorbed (A) and the concentration (C) of the absorbing sample. This relationship is called the Lambert Beer law as given in equation 2.4.

$$A = \varepsilon . c . L \qquad (2.4)$$

Where,

ε : Extinction coefficient (specific to each substance) (cm^{-1})

L : Path Length (cm)

A : Absorbance (no units)

c : Concentration (M)

Moreover, absorbance is proportional to (T) which is the light transmitted through the sample. Inside the spectrophotometer a Xenon lamp directs beam of light through the cuvette and the sample in the cuvette absorbs particular wavelengths. Transmitted light, the light which is not absorbed, passes through the cuvette and is first diffracted and then directed onto the detector. The spectrograph shows the absorbance value of that sample for the whole range of wavelengths within the ultraviolet and visible regions. By using the calibration curve which shows absorbance at a particular wavelength against concentration, concentration of a sample can be determined.

In this study, UV-Vis was one of the core analysis because it helped to show how much effective the gating mechanism was. The brand of the instrument is Agilent Technologies UV-Vis Spectrophotometer.

3. MATERIALS AND METHODS

3.1. Materials

Tetronic 1107 and T904 were endowed by BASF (North America). Pluronic F127, sodium Hydroxide (NaOH), hexadecyl trimethyl ammonium bromide (CTAB), trizma base, N-(3-Dimethylaminopropyl)-N′-ethylcarbodiimide hydrochloride (EDAC) and arginine were purchased from Sigma. Tetraethyl orthosilicate (TEOS), triethoxy(octyl)silane (OTES), (3-Aminopropyl)triethoxysilane (APTES) ans succinic anhydride were obtained from Aldrich. Anhydrous acetonitrile and anhydrous dioxane were provided from Sigma-Aldrich. Acetone (Emsure), n-Hexane (Emplura), diethyl ether (Emsure), 1,2-ethylenediamine, tetrahydrofuran (THF) (Emplura), 25% ammonia solution (Emprove), dimethylformamide (DMF) (Emsure), ethanol (Emsure), 4-dimethylamino pyridine (DMAP) and triethylamine (TEA) were obtained from Merck KgaA. N,N'- Carbonyldiimidazole (CDI) is provided from Acros Organics. Curcumin (Curfen) is purchased from Abfen Farma. Except Tetronic T1107 and Pluronic F127, all chemicals were used as received. All solutions prepared with deionized water.

3.2. Synthesis of Mesoporous Silica Nanoparticles (MSNs)

The well-studied Ströber process was used to synthetize MSNs [37]. The details of the synthesis steps for each type of MSN are listed below:

3.2.1. Synthesis of MCM-41

Two types of CTAB templated MCM-41 were produced, in one of them F127 was used as dispersion stabilizer [38]. For the first one (without F127), 2M NaOH solution was prepared by simply dissolving 0.2 g Sodium hydroxide (NaOH) pellet in 2.5 ml water. 1.75 ml of NaOH solution was added into 240 ml of water. 500 mg of hexadecyl trimethyl ammonium bromide (CTAB) was slowly (in approximately 2 hours) added into the solution to avoid foam formation.

The solution was stirred at 300 rpm until it is clear indicating complete dissolution of CTAB. Temperature was adjusted to 80℃ by using temperature controller IKA C-MAG HS 7. 2.5 ml of Tetraethyl orthosilicate (TEOS) was added dropwise, once the temperature reached 80°C. Stirring rate was set to 500 rpm to create turbulence at the beginning of the reaction. After 30 seconds, stirring rate was reduced to 300 rpm. Once the solution color turned white, the reaction was stirred for additional 2 hours under the same conditions. After 2 hours the reaction was allowed to reach equilibrium overnight.The particles were collected by centrifuging (Sigma 3-16PK) at 4500 rpm for 20 minutes, washing with water for 3 times, then drying in the oven at 70°C overnight. Dried particles were calcined at 550°C for 5 hours to remove the surfactant.

In the second one (with F127), 200 mg hexadecyl trimethyl ammonium bromide (CTAB) was dissolved in 95 ml of water. 5 mg/ml F127-water solution and 2 M NaOH solution were prepared. 1 ml of F127 solution and 0.7 ml of NaOH solution were added simultaneously into CTAB solution. By using a temperature controlled stirrer, the temperature of the mixture was set to 80°C. The solution was stirred vigorously (at around 600 rpm). When the temperature reached 80°C, 1.2 ml of TEOS was added to the solution rapidly. The reaction mixture was stirred for 2 hours, then the solution was cooled down to the room temperature. Particles were collected and calcined as described above.

3.2.2. Synthesis of Hydrophobic Mesoporous Silica Nanoparticles (hMSN)

200 mg of CTAB and 6 mg of F127 were dissolved in 96 ml of water. 0.7 ml of 2M NaOH solution was added into first solution. While stirring at 600 rpm, reaction was heated up to 80℃ and rapidly 1.5 ml of TEOS was added. In a few minutes, the reaction became turbid indicating MSN formation. 0.25 ml Triethoxy(octyl)silane (OTES) was dissolved in 10 ml tetrahydrofuran (THF). After 30 minutes, OTES-THF solution was added into the reaction solution to form hydrophobic layer around the particles. Solution was stirred for additional 2.5 hours under the same conditions. Particles were collected by centrifugation at 4500 rpm for 20 minutes and washed with ethanol. Particles were dispersed in 50 ml ethanolic ammonium nitrate solution (20 mg/ml) in order to remove surfactants. This solution was stirred at 60℃ for 30 minutes. Particles

were collected with centrifugation then ammonium nitrate treatment was repeated one more time. Collected particles were washed with ethanol three times then dried at 60℃ overnight.

3.2.3. Synthesis of Amino functionalized Mesoporous Silica Nanoparticles (MSN-NH_2)

A mixture was prepared by using 5.84 ml ethanol and 7.716 ml ammonia solution (25 % w/v). 0.1 g of CTAB was very slowly added into the solution (approximately in 2.5 hours). After CTAB was dissolved in the solution, 0.3 ml of TEOS and 0.1 ml (3-aminopropyl)triethoxysilane (APTES) were added to the solution. Solution was sonicated by using a sonoreactor at 20 Hz, 100 W for 30 minutes. Mixture was stirred for additional 20 hours at room temperature to obtain homogenous suspension. Particles were collected by centrifugation at 4500 rpm for 20 minutes. Collected particles were washed once with 70% ethanol-water mixture then recollected. Particles were dried overnight at 60℃. The dried particles were washed and sonicated with 1% (w/v) ammonium nitrate solution at 50℃ to completely remove the surfactant. Washed particles were collected and dried under vacuum or in oven at 50℃.

3.2.4. Synthesis of Carboxylic acid functionalized Mesoporous Silica Nanoparticles (MSN-COOH)

330 mg of amine modified mesoporous silica nanoparticles were dissolved in 10 ml THF and dispersed by using a sonicator for 15 minutes. 42 mg (0.417 mol) Succinic Anhydride was dissolved in 417 ml dimethylformamide (DMF) and poured into THF-MSN solution. The mixture was stirred at room temperature for additional 16 hours, then it was precipitated in 250 ml diethyl ether. The particles were collected by centrifugation at 4500 rmp for 20 minutes. Collected particles were dissolved in 5 ml ethanol and precipitated in 150 ml diethyl ether once more. Particles were collected again and dispersed in 10 ml ethanol. Particles were stored in ethanol.

3.3. Synthesis of Amine ended T1107 (T1107-NH2)

Aminated Tetronic T1107 were prepared in two steps.

3.3.1. Synthesis of CDI-activated Tetronic T1107 (T1107-CDI)

T1107-CDI were synthesized based on the procedure reported by Zhang *et al*., (2011) with slight modifications. 10 g T1107 was purified by dissolving in 200 ml acetone and precipitating into 600 ml (excess amount) of cooled hexane. Solution was dried under vacuum (Christ RVC 2-18) at 30℃, first for 20 minutes followed by subsequent 35 minutes. Purified Tetronic 1107 was collected. 2.5 g of purified Tetronic was dissolved in 5 ml anhydrous acetonitrile under nitrogen environment. This solution was added dropwise into the 2.16 g (excess amount) N,N'-Carbonyldiimidazole (CDI) in 20 ml dry acetonitrile during 2 hour period under nitrogen environment. The mixture was stirred for an additional 4 hours, then concentrated in rotary evaporator (IKA RV-10 digital and IKA HB-10 digital) at 27℃. The residue was poured into excess amount of diethyl ether to remove unreacted CDI and collected by the rotary evaporator at 18℃. This step was repeated three times. Purified T1107-CDI solution was dried under vacuum and collected as slightly yellow solid material.

3.3.2. Synthesis of amino terminated Tetronic 1107 (T1107-NH2)

0.205 g of T1107-CDI was dissolved in 5 ml of anhydrous acetonitrile under nitrogen environment. Solution was added dropwise into 0.56 ml 1,2 ethylenediamine during 2 hour period at room temperature under nitrogen environment. The mixture was stirred for 24 hours. Unreacted ethylenediamine was removed by the rotary evaporator at 25℃. The residue was precipitated in cold diethyl ether. If necessary, above procedure was repeated once more. The mixture was filtered, then dried by vacuum dehydration, and collected as white (slightly creamy) solid material.

3.4. Synthesis of amine ended F127

Aminated Pluronic F127 were synthesized in two steps.

3.4.1. Synthesis of CDI-activated Pluronic F127 (F127-CDI)

F127-CDI were synthesized with the same procedure as described in Section 2.3. Purification steps are competely same with the Section 2.3. Purified Pluronic F127 was collected. 12.6 g (1 mmol) of purified Pluronic F127 was dissolved in 15 ml dry acetonitrile under nitrogen environment. This solution was added dropwise into the mixture of 1.62 g (10 mmol) N,N'- Carbonyldiimidazole (CDI) in 15 ml dry acetonitrile during 2 hour period under nitrogen environment. Mixture was kept stirred for an additional 4 hours. The mixture was concentrated in rotary evaporator under 27℃. Residue was collected as aforementioned in Section 2.3.

3.4.2. Synthesis of amino terminated Pluronic F127 (F127-NH_2)

12.7 g (1 mmol) of F127-CDI was dissolved in 15 ml of dry acetonitrile. Solution was added into 10 ml of 1,2 ethylenediamine during 2 hour period under room temperature and nitrogen environment. Mixture was kept stirred for 24 hours. Unreacted ethylenediamine was removed by rotary evaporator (25℃). Residue was poured into excess amount of diethyl ether to obtain white precipitate. This step was repeated three times. The mixture was dried by vacuum dehydration, and collected as slightly yellow-white solid material.

3.5. Synthesis of carboxylated T1107 (T1107-COOH)

Carboxyl functionalized MSNs are synthesized by following the procedure reported by Park *et al.*, (2010) 6 g of Tetronic T1107 was dissolved in 72 ml of anhydrous dioxane at 30℃ under nitrogen atmosphere. 0.244 g of 4-dimethylamino pyridine (DMAP) and 0.279 ml Triethylamine (TEA) were dissolved at the same time in anhydrous dioxane. 9.6 ml of TEA-

DMAP solution was added into the T1107 solution prepared above. Whole mixture was stirred for 15 minutes to activate the end group of Tetronic T1107. Succinic anhydride solution was prepared by dissolving 0.200 g succinic anhydride in dioxane. Then, succinic anhydride solution was added to the activated mixture. The reaction mixture was stirred for additional 24 hours under the same conditions. Dioxane was removed by using rotary evaporator at 40℃. Residue was precipitated in cold diethyl ether twice. By using filtration and vacuum, the product was dried.

3.6. Synthesis of Pluronic/Tetronic Gated MSNs by chemical methods

Crosslinking of functionalized MSNs and copolymers is achieved by following the article by Bhattacharyya *et al*., (2012).

3.6.1. Crosslinking of carboxylated MSN and aminated Tetronic T1107

0.9 g of aminated Tetronic (T1107-NH_2) was dissolved in 2.5 ml Tris Buffer (pH 7.4). 50 mg of carboxylated mesoporous silica nanoparticles (MSN-COOH) was dissolved in this solution and 40 mg of N-(3-Dimethylaminopropyl)-N′-ethylcarbodiimide hydrochloride (EDAC) was added as a crosslinking agent. The mixture was stirred for 1 hour at room temperature. The particles were collected and washed several times to remove unreacted T1107-NH_2 and EDAC. Collected particles were dried at 37℃ in oven for 2 days or under vacuum.

3.6.2. Crosslinking of carboxylated MSN and aminated Pluronic F127

0.378 g of aminated Pluronic (F127-NH_2) was dissolved in 2.5 ml Tris Buffer (pH 7.4). 50 mg of carboxylated mesoporous silica nanoparticles (MSN-COOH) was dissolved in this solution and 40 mg of N-(3-Dimethylaminopropyl)-N′-ethylcarbodiimide hydrochloride (EDAC) was added as the crosslinking agent. The mixture was stirred for 1 hour at room temperature. The particles were collected and washed several times to remove unreacted F127-NH_2 and EDAC. Collected particles were dried at 37℃ for 2 days in oven or under vacuum.

3.6.3. Crosslinking of aminated MSN and carboxylated Tetronic T1107

34.3 g of aminated mesoporous silica nanoparticles (MSN-NH_2) was dissolved in 2.5 ml Tris Buffer (pH 7.4). 0.9 mg of carboxylated Tetronic T1107 (T1107-COOH) was dissolved in this solution and 40 mg of N-(3-Dimethylaminopropyl)-N′-ethylcarbodiimide hydrochloride (EDAC) was added. The mixture was stirred for 1 hour at room temperature.The particles were collected and washed several times to remove unreacted materials. Collected particles were dried at 37℃ for 2 days in the oven or under vacuum.

3.7. Synthesis of Pluronic/Tetronic Gated MSNs by physical methods

Physical gating mechanism for Pluronic and Tetronic is constructed by following the article written by Yildirim *et al*., (2013).

3.7.1. Tetronic T1107 Capping of Hydrophobic MSN

1200 mg of Tetronic T1107 was dispersed in 200 ml water to make (6 mg/ml) T1107 solution. 100 mg of hydrophobic mesoporous silica nanoparticles was added into T1107 solution. The mixture was sonicated for 15 minutes then stirred for 1 hour, and the particles were collected. Again, 200 ml of 6 mg/ml T1107 solution was prepared. Collected particles were added into this solution. The mixture was sonicated for 15 minutes and stirred for 1 hour. Particles were collected and washed several times to remove excess T1107.

3.7.2. Tetronic T904 Capping of Hydrophobic MSN

540 mg of Tetronic T904 was dispersed in 200 ml water to make (2.7 mg/ml) T904 solution. 100 mg of hydrophobic mesoporous silica nanoparticles was added into T904 solution. The mixture was sonicated for 15 minutes and stirred at 300 rpm for 1 hour. The particles were collected. 200 ml of 2.7 mg/ml T904 solution was prepared again. Collected particles were added into this solution. The mixture was sonicated for 15 minutes and stirred for 1 hour. The particles were collected and washed several times to remove excess T904.

3.7.3. Pluronic F127 Capping of Hydrophobic MSN

1000 mg of Pluronic F127 was dispersed in 200 ml water to make (5 mg/ml) F127 solution. 100 mg of hydrophobic mesoporous silica nanoparticles was added into F127 solution. The mixture was sonicated for 15 minutes and stirred for 1 hour. Collected particles were added into 200 ml of 5 mg/ml F127 solution. The mixture was sonicated for 15 minutes and stirred for 1 hour. The particles were collected and washed several times to remove excess F127.

3.8. Toxicity Experiments

All equipments were sterilized by using autoclave (ALP CLG). *Saccharomyces cerevisiae* were grown at 28 ℃ and 180 rpm in shaker overnight. Yeasts were washed at 9000 rpm 4 ℃ for 10 minutes in yeast solution, then they were washed three times with 1X PBS at 9000 rpm 4 ℃ for 1 minute. At two different concentration (250 and 500 µg/L), for 5 types of nanoparticles, solutions were prepared by using 1X PBS. Yeast solutions was prepared by taking approximately 1 million cell in 1 ml yeast solution, then nanoparticle solution was added into mixture. Nanoparticle and yeast solution was shaken at 60 rpm for 1 hour. Mixed solution was diluted at 1/100 and 1/200 with PBS. 100 ml of the diluted solutions were added into agar plates. Then, agar plates were covered with parafilm and incubated at 30 ℃ for 3 days. After 3 days, the formed colonies were counted.

4. RESULTS AND DISCUSSION

4.1. Physical Gating of MSNs

In this method, by taking the advantage of hydrophobic attraction between the copolymers and surface modified mesoporous silica nanoparticles, copolymer gating of MSN surface is achieved. Also, bare MSNs are produced as a control group.

4.1.1. Synthesis and Characterization of MSN

Bare mesoporous silica nanoparticles (MCM-41) are synthesized by following the protocol given in section 3.2.1. Similarly, Octyl modified mesoporous silica nanoparticles, i.e., hydrophobic mesoporous silica nanoparticles (hMSN) are produced as described in section 3.2.2. In brief, surface modification is achieved through the addition of OTES to the reaction mixture. As demonstrated in Figure 1, hydrophobic MSNs float on the surface of water while bare MSNs slightly disperse but mostly sink to the bottom of water, indicating successful surface treatment for hMSNS.

(a) (b)

Figure 4. 1. (a) hMSN in water (b) Bare MSN in water.

In Figure 4.2 and 4.3, SEM images of bare MSNs and STEM images of hMSNs are demonstrated respectively. Since hMSNs are not soluble in water, STEM analysis are made by dissolving hMSNs in ethanol. When STEM analysis of hMSNs are made in water, they show adherent and irregular patterns (results not shown). Moreover, particle diameter of bare MSNs is found as approximately 50-60 nm and the particle diameter of hMSNs is around 80 nm as illustrated in Figure 4.2 and Figure 4.3 respectively. Both NPs have roughly spherical geometry, but hMSNs have more size variation.

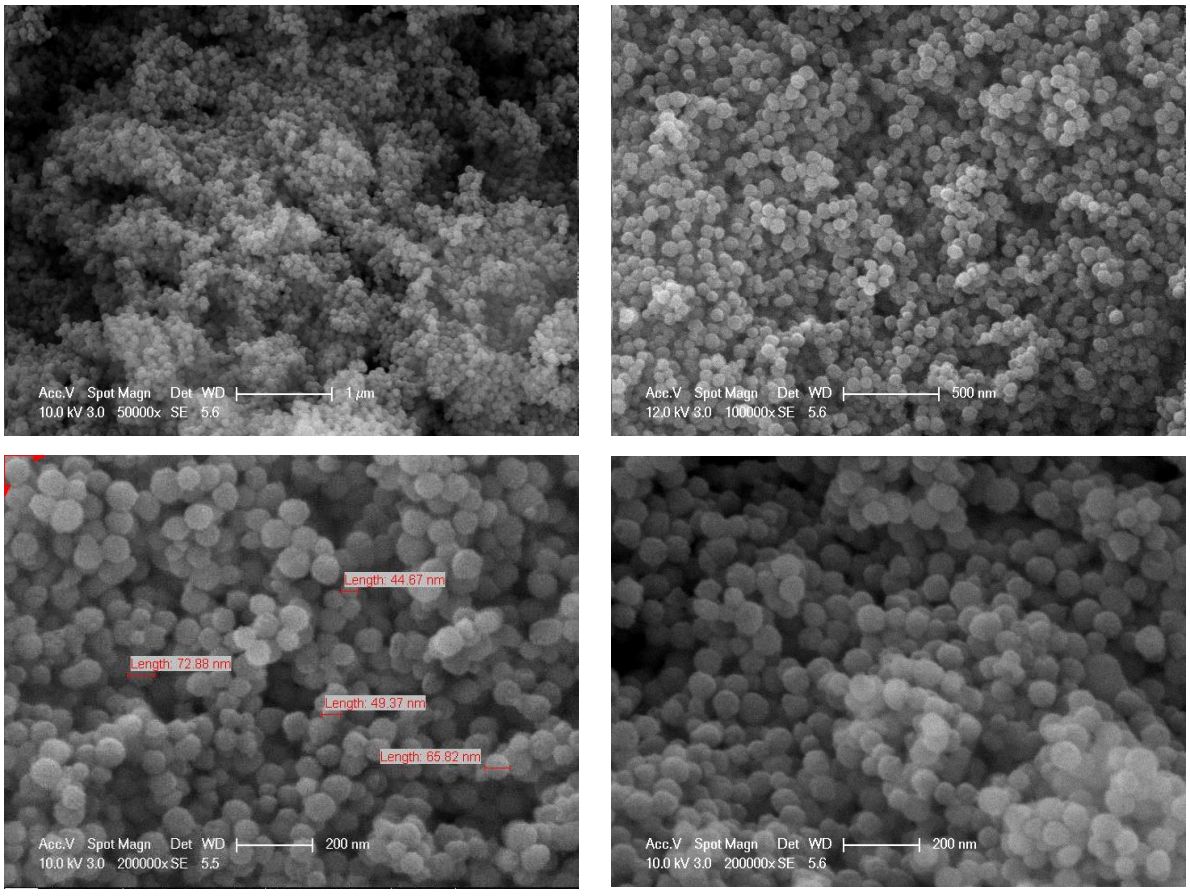

Figure 4. 2. SEM images of bare MSNs.

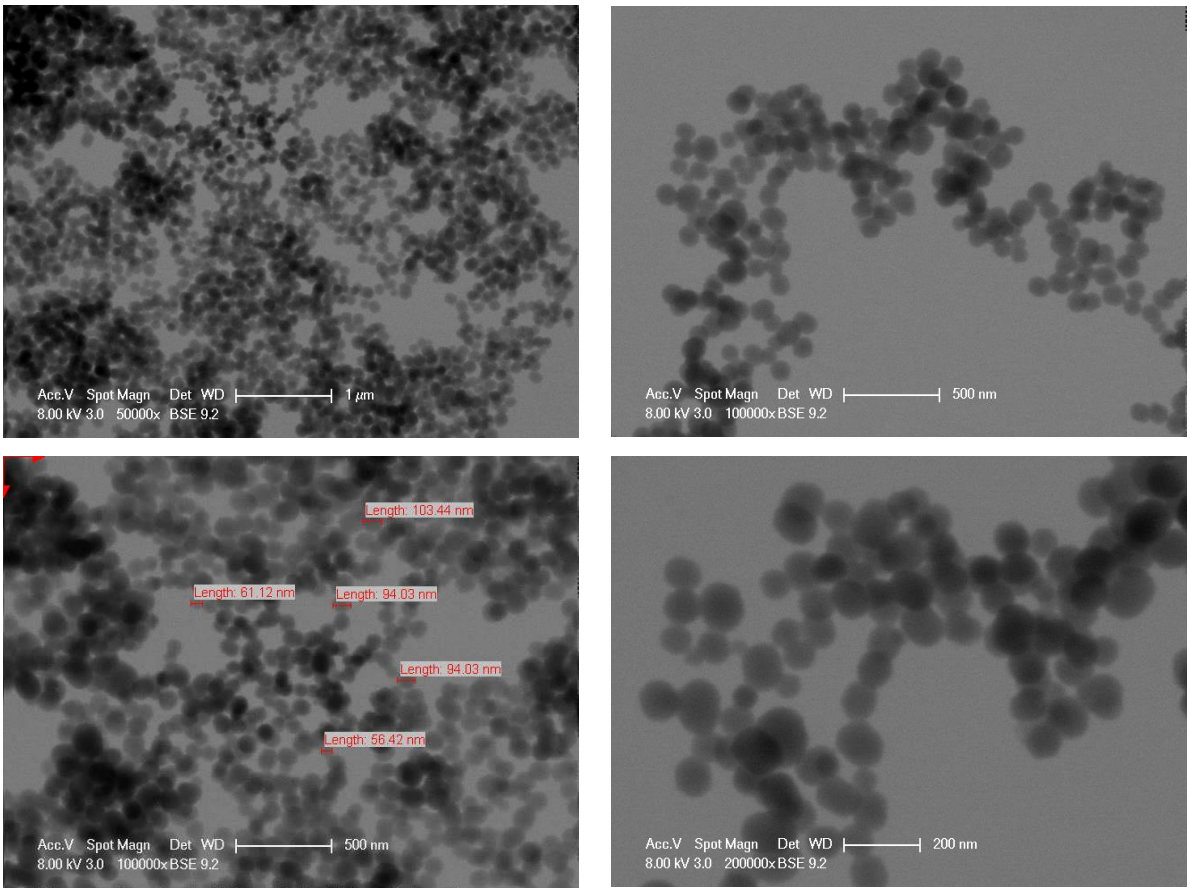

Figure 4.3. STEM images of bare hMSNs in ethanol.

4.1.2. Pluronic/Tetronic coated hMSN

Hydrophobic layer around the particles provide hydrophobic interaction between the hydrophobic poly-propylene oxide (PPO) blocks of Pluronic/Tetronic copolymers and the nanoparticle surface [5]. After gating the MSNs by the copolymers physically through these hydrophobic interactions, the particles are observed to disperse in water. Dispersion in water is enabled by poly-ethylene oxide (PEO) end of the copolymer which has hydrophilic nature compatible with water. Also, this provides an evidence of hydrophobic nanoparticle surface being coated successfully. Being soluble in water is important in terms of biocompability.

4.1.2.1. Tetronic T1107 coated hydrophobic mesoporous silica nanoparticles. Tetronic T1107 is highly hydrophilic due to its PEO/PPO ratio (3.0) which enables to form a stable structure within aqueous media. As it is illustrated in Figure 4.4, PPO part of the Tetronic T1107 interacts with the hydrophobic surface of hMSNs. As mentioned before, PEO is the part of the copolymer which provides the stability and solubility in water. Therefore, this method is a promising way to keep the cargo inside the pores while hiding the NP from the immune system of the body. Also, Tetronic serve as pH sensitive gate to prevent premature release, and provide stimuli responsiveness.

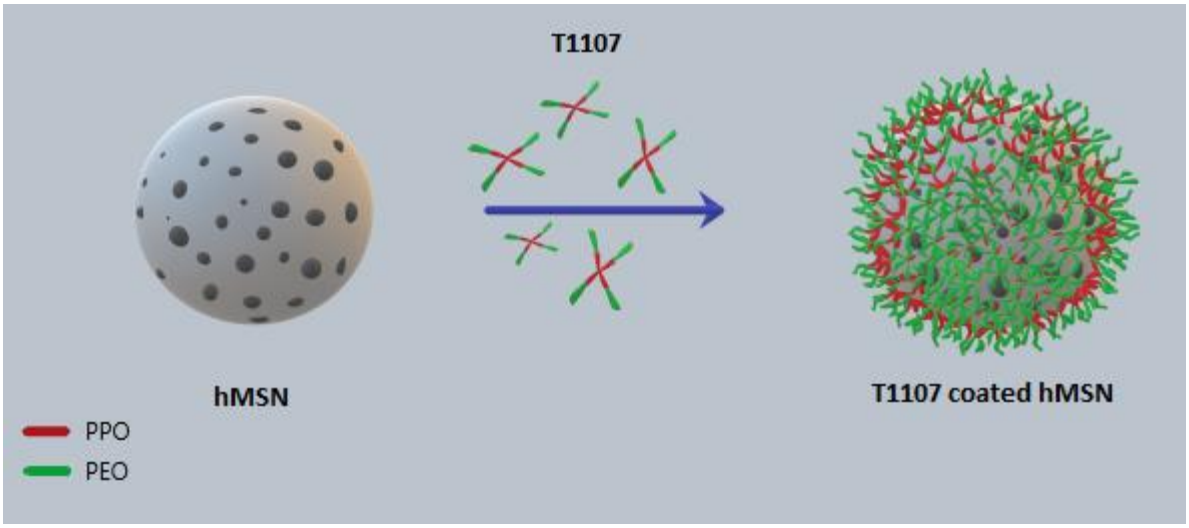

Figure 4.4. Schematic of T1107 coated hMSNs.

After coating of hMSNs with Tetronic T1107 the particles are characterized by STEM analysis. No significant particle size change is observed between bare MSNs and T1107 coated hMSNs as demonstrated in STEM images in Figure 4.5. Bare particle diameters of hMSNs are roughly between 50-100 nm (mostly 80 nm) and the particle diameters of Tetronic T1107 coated hMSNs are around 80 nm and more. The reason for similar diameters observed in STEM is that Tetronic T1107 shrink on the surface of hMSN as it is dried, limiting its visibility under STEM.

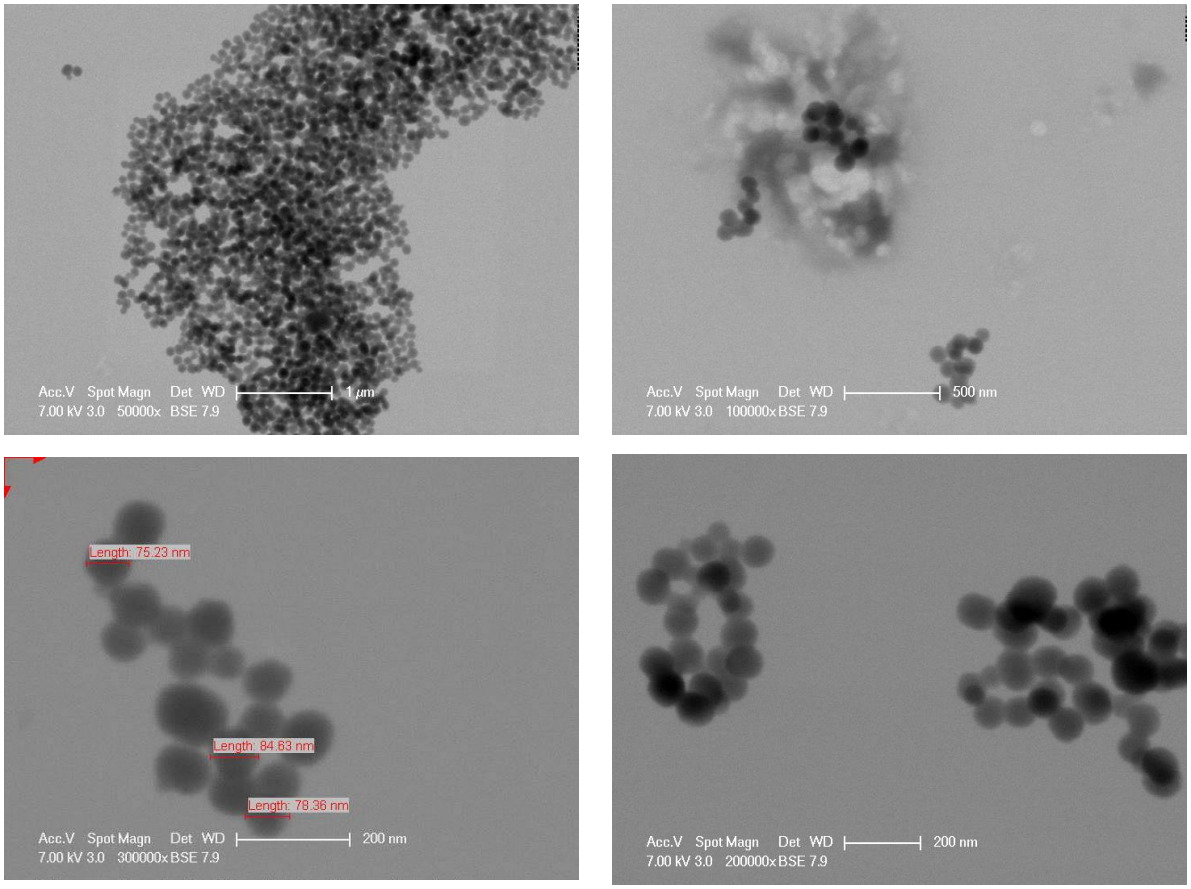

Figure 4.5. STEM images of T1107 coated hMSNs.

On the other hand, with DLS analysis (Figure A.1), Tetronic T1107 coated hMSNs' average particle diamater is found as 306 nm with the 'number' mode. The discrepancy between STEM and DLS measurements has occurred due to the differences between the techniques. In DLS measurements, first the diffusion coefficient and from that hydrodynamic radius is calculated. Therefore, in this technique the result is associated with the hydrodynamic behavior of molecules. DLS analysis is also performed in aqueous media enabling Tetronic T1107 arms to stretch and swing. However, STEM analysis is made by letting the aqueous media to dry on copper grids. As the particles get dried, Tetronic T1107 arms shrink and attach over the nanoparticle surface.

In order to understand the efficiency of the gating mechanism, diffusion experiments are performed. For this purpose, hMSNs are loaded with curcumin, then, curcumin loaded hMSNs are coated with copolymers as described in Section 3.7.1. Curcumin is selected as cargo molecule due to its hydrophobic nature which is compatible with surface of hMSNs. After the coating process, cargo release rates in PBS are examined for the following temprature and pH conditions: at 25℃ , 37℃, 43℃ and pH 7.4 as well as at 37℃ and pH 4.8. Different temperature and pH values are chosen to observe temperature and pH effect on the gating mechanism separately, in accordance with the physiological conditions. According to Tannock *et al*., (1989), cancer cell environment is usually more acidic. Tetronic T1107 has pKa values of 5.6 and 7.9 which means that gating mechanism is activated at or below pH 5.6. Moreover, PBS is selected as the aqueous media due to its pH value of 7.4 which is close to human body environment. Also it is most commonly used non-toxic and isotonic biological media.

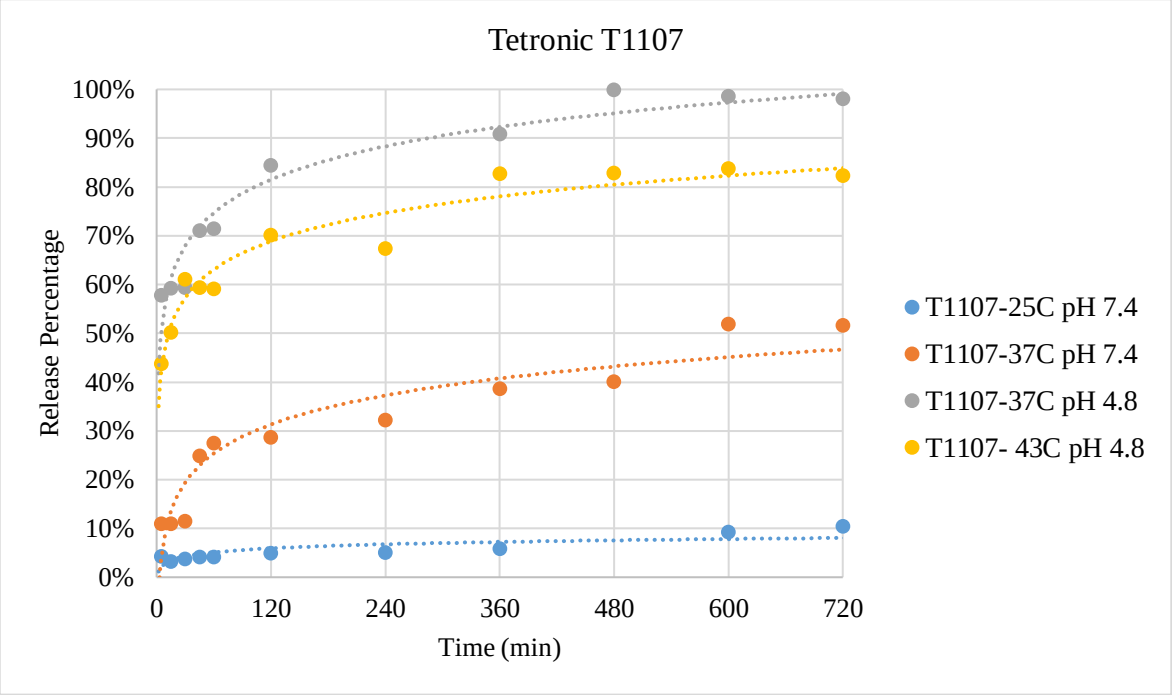

Figure 4.6. Release of curcumin from Tetronic T1107 coated hMSNs.

In Figure 4.6, the release data of curcumin is demonstrated at different temperature and pH conditions. It is observed that at 37℃ and pH 4.8 the release rate of curcumin is the most. This phenomenon meets with the expectation of having the highest release rate at acidic environment. For Tetronic T1107, it is expected from the polymer to stretch and release the cargo as pH decreases [43]. Moreover, melting point of T1107 is approximately 50 ℃. Therefore, the gating mechanism cannot work at high temperatures with the physical attachment method.

4.1.2.2. Pluronic F127 coated hMSNs. Pluronic F127 has high hydrophilic nature (PEO/PPO ratio is 3.08) similar to T1107. However, Pluronic F127 does not have an X shape. Instead, it has a rod shape structure with two PEO blocks connected to a PPO block as illustrated in Figure 4.7. Similar to synthesis approach of Tetronic T1107 capped MSNs (section 4.1.2); PPO part of the Pluronic F127 sticks to the hydrophobic surface of hMSN and PEO part of the Pluronic F127 is repelled away from the surface of nanoparticle. PEO extensions of Pluronic F127 provide hydrophilic nature to the nanoparticle.

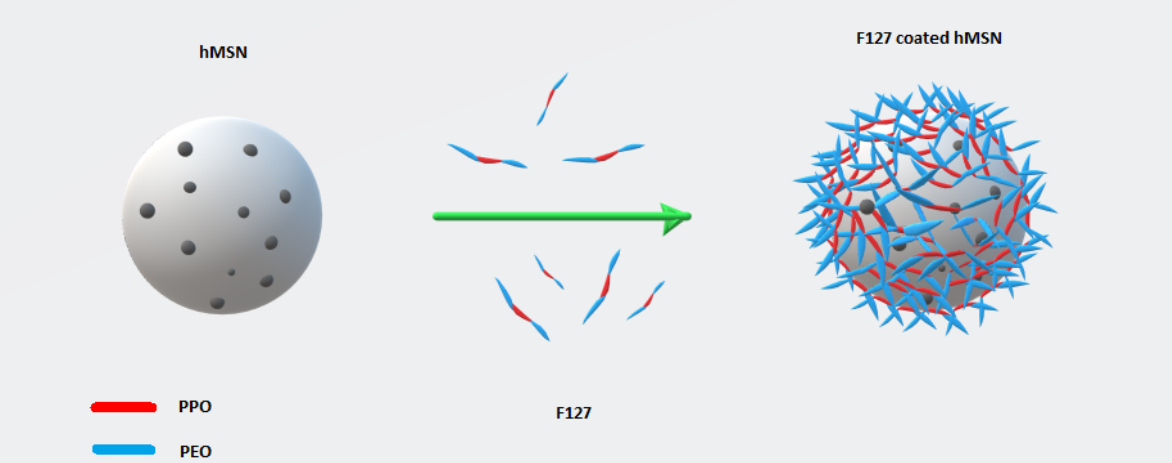

Figure 4.7. Schematic of F127 coated hMSNs.

In Figure 4.8, STEM images of Pluronic F127 coated hMSNs are demonstrated. Coated particle sizes are roughly between 80-120 nm (mostly 100 nm). Also, as it is seen in STEM results, Pluronic F127 coated nanoparticles have spherical shape. From DLS measurements, particle diameters are found as 718 nm. The difference between STEM and DLS results is due to same reason explained for Tetronic T1107 in Section 4.1.2.

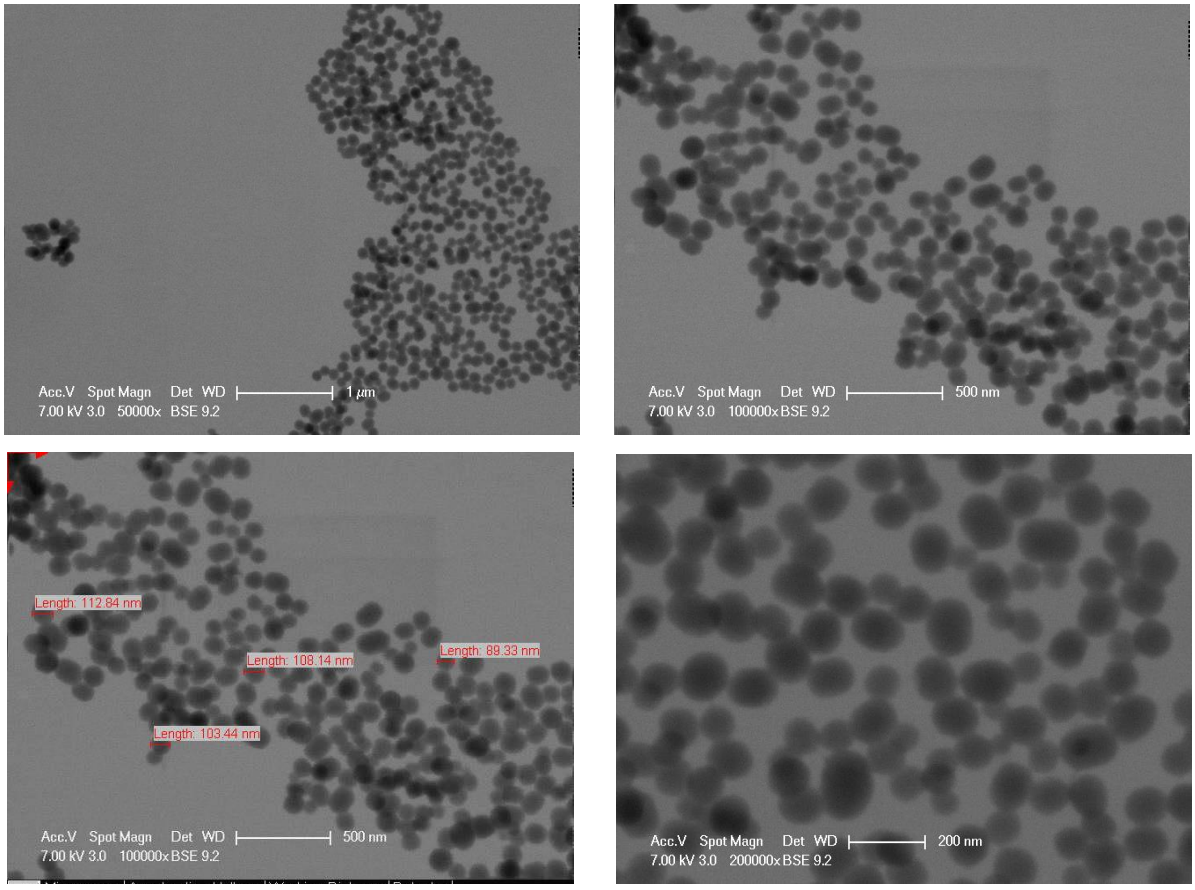

Figure 4.8. STEM images of F127 coated hMSNs.

In Figure 4.9, curcumin release data for Pluronic F127 coated hMSNs is given. The most release occurs at 43℃ and pH 7.4. This is followed by the release data at 37℃ and pH 4.8 as well as at 37℃ and pH 7.4. However, at 25℃ and pH 7.4, curcumin release is relatively low which is contradicted with the expectations. According to Yildirim *et al.*, (2013) research, F127 capped nanoparticles release its cargo molecule more at low pH value which is in coherence with the results in Figure 4.9. As temperature increases Pluronic F127 tend to melt at 53-57℃

and leave the nanoparticle surface. This distrupts the gating mechanism and causes the release of curcumin molecules more.

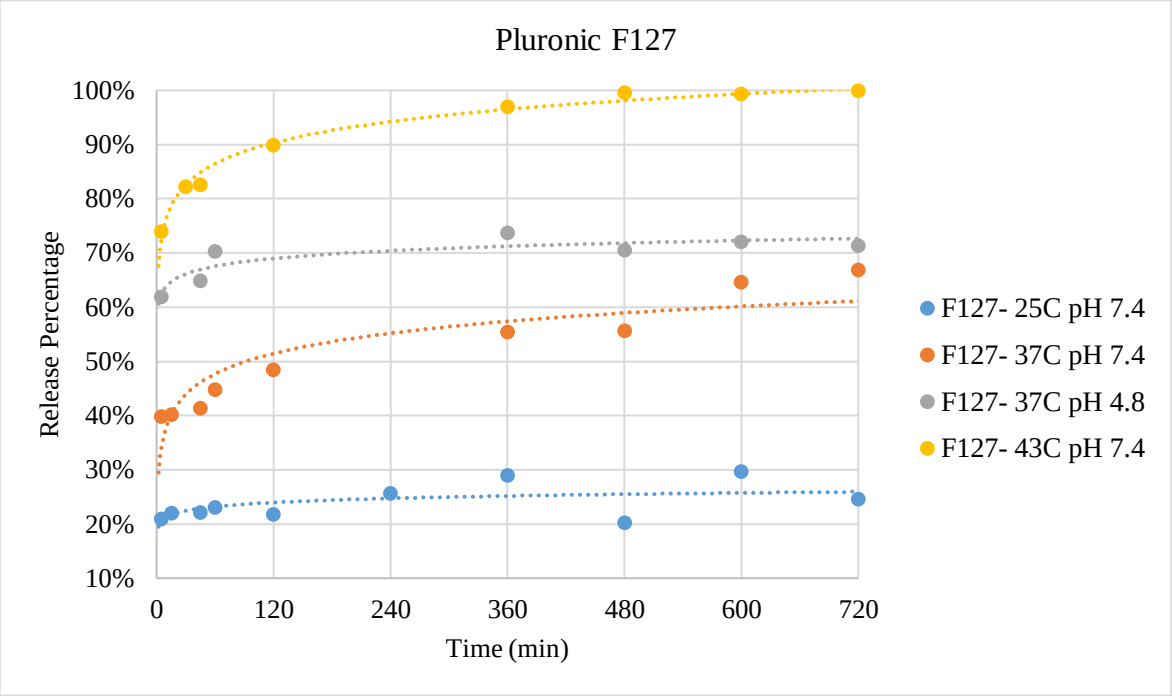

Figure 4.9. Release of curcumin from Pluronic F127 coated hMSNs.

4.1.2.3. Comparison of T1107 and F127 coated hMSNs. Taking into consideration the STEM and DLS results, the sizes of hMSNs coated with Pluronic F127 are bigger than the ones coated with Tetronic T1107. This results from the large number of PEO units in Pluronic F127 compared to Tetronic T1107 as shown in Figure 4.10. While Pluronic F127 has 100 average PEO units and 65 PPO Units, Tetronic T1107 has 62 PEO and 20 PPO units in one arm [41,45].

(a)

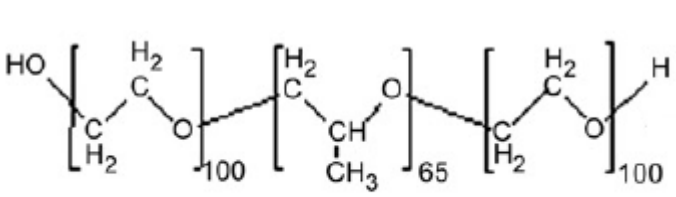

F127

(b)

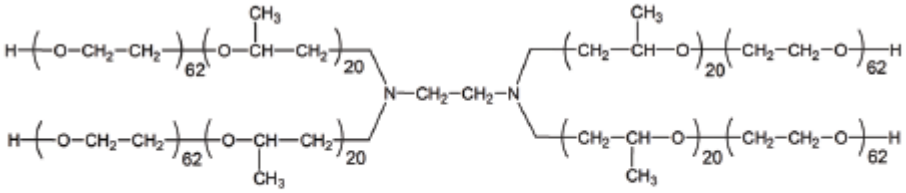

T1107

Figure 4.10. Structure of (a) T1107 and (b) F127 [40].

Moreover, both type of copolymers (T1107 and F127) have released the cargo more at high temperatures. As temperature decreases, both T1107 and F127 result in lower release rates.

4.2. Chemical Gating of MSNs

4.2.1. Carboxylated Tetronic T1107 gated Aminated MSNs (T1107COOH-MSNNH2)

4.2.1.1.Synthesis and Characterization of Aminated MSN (MSNNH2). Aminated MSNs are synthesized by following the protocol reported by Kim *et al*., (2012). The synthesis steps are similar to those of MCM-41 as mentioned in section 3.2.1. The only difference is the addition of APTES to the reaction mixture which results in the amination of the surface as illustrated in Figure 4.11.

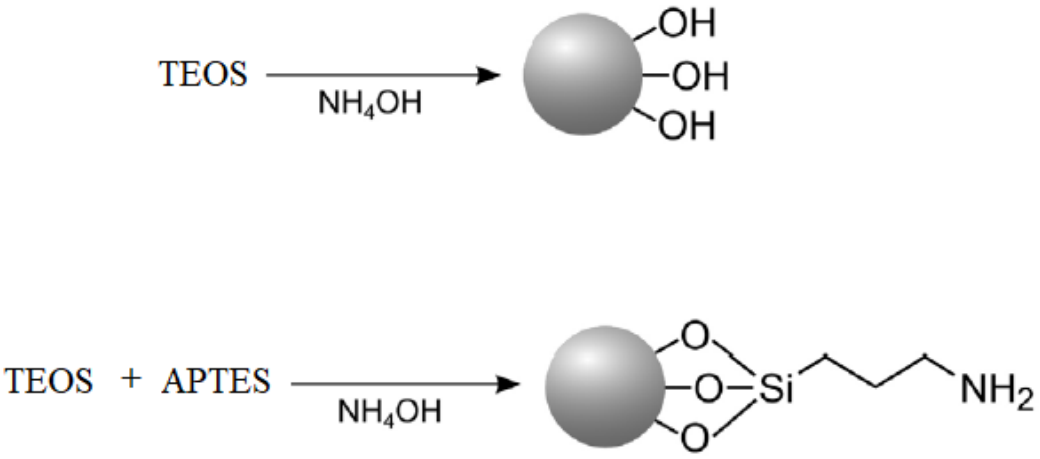

Figure 4.11. Schematic of amination process for MSN.

In Figure 4.12, STEM images of $MSNNH_2$ are shown. The average particle diameter is roughly between 120-300 nm and the particles have spherical geometry in general.

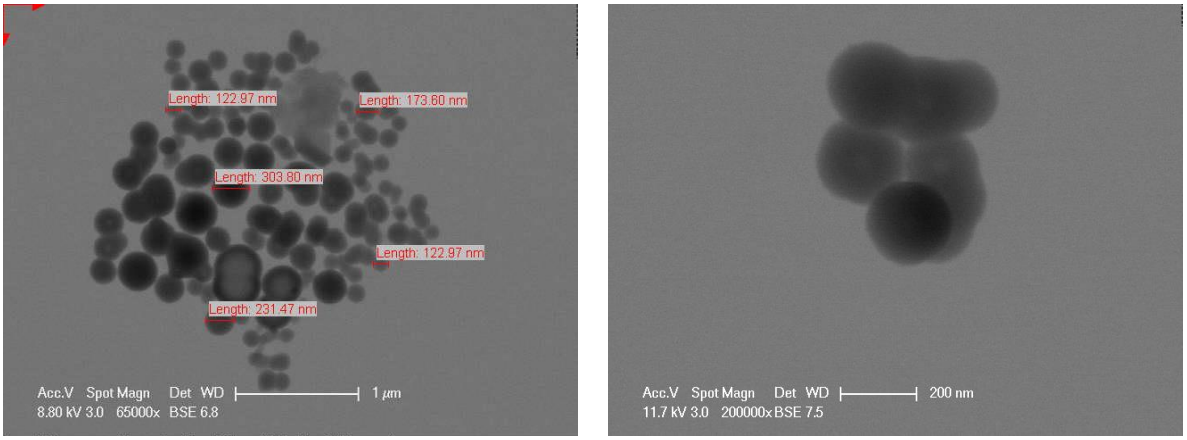

Figure 4.12. STEM images of $MSNNH_2$.

Functionalization of MSNs with amine groups is verified by FTIR analysis. In Figure 4.13, an amine peak appears at 1540 cm^{-1}. A broad peak occurs between 2800 to 3300 cm^{-1} as these peaks represents characteristic of N-H bending and stretching vibrations of primary amines.

These results are in agreement with the findings reported by Suteewong *et al.*, (2012) where the amine peaks are observed at 1560 cm^{-1} and N-H bending/stretching vibrations are detected between 2800-3300 cm^{-1} range.

Moreover as illustrated in Table 4.1 and Figure A.3, aminated mesoporous silica nanoparticle is positively changed and its zeta potential value is +39.90.

4.2.1.2. Synthesis and Characterization of Carboxylated Tetronic T1107 (T1107COOH). Carboxylated Tetronic T1107 is produced by following the protocol reported by Park *et al.*, (2010).

As illustrated in Figure 4.14, -OH ends of the Tetronic T1107 are functionalized by using succinic anhydride accompanied with anhydrous dioxane and TEA. Also, DMAP endows the reaction to be carried out at room temperature as catalyst [46].

Addition of succinic anhydride has an important role. If succinic anhydride is added at the beginning of the reaction, then only one side of the copolymer (-OH end) is altered. However, if succinic anhydride is added after activation of Tetronic T1107, all –OH ends of Tetronic T1107 can be functionalized successfully.

In this work succinic anhydride is added after the activation of Tetronic T1107 in order to functionalize all –OH ends of Tetronic T1107.

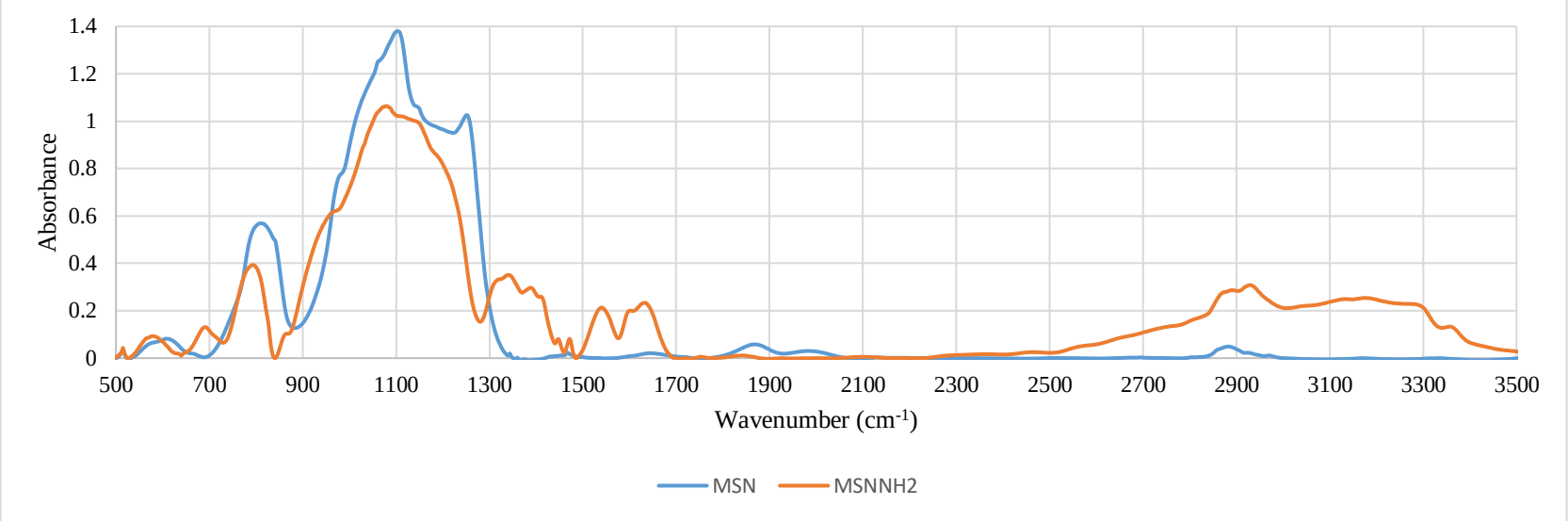

Figure 4.13. FTIR spectra of MSN and $MSNNH_2$.

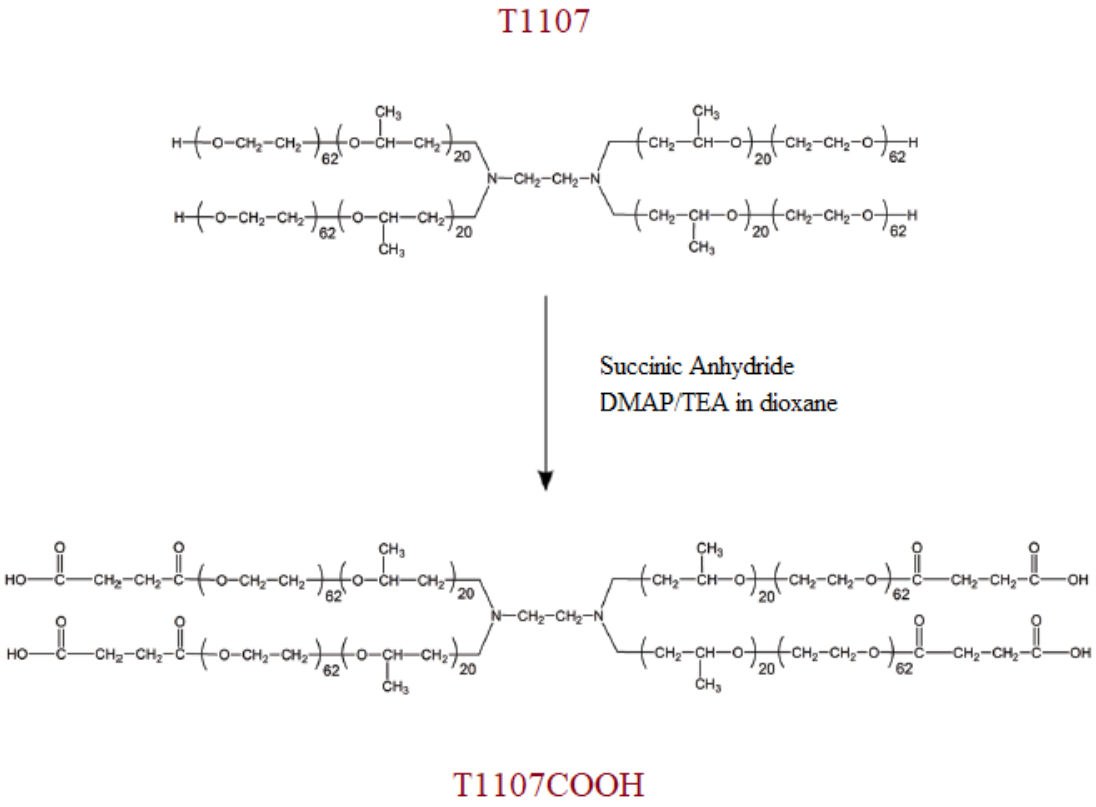

Figure 4.14. Schematic of carboxylation process for Tetronic T1107.

Functionalization of T1107 with carboxyl groups is verified by FTIR analysis. A peak associated with carbonyl stretching vibration should appear at or around 1750 cm^{-1} according to Park *et al.*, (2010).

In Figure 4.15, a peak is observed at 1740 cm^{-1} demonstrating successful carboxylation of Tetronic T1107.

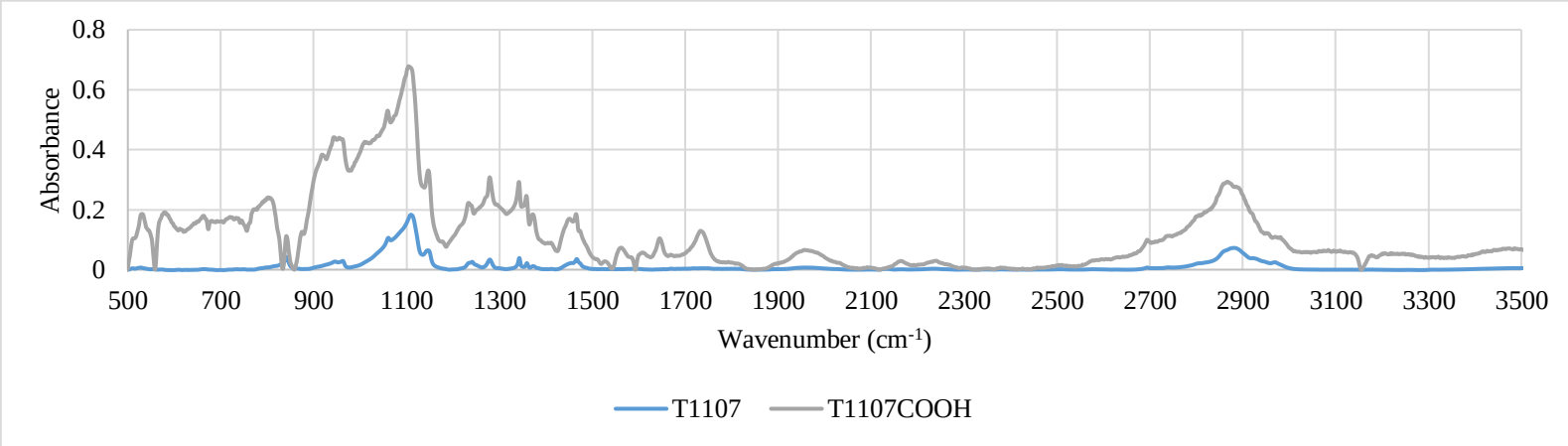

Figure 4.15. FTIR spectra of T1107 and T1107COOH.

4.2.1.3. Synthesis and Characterization of T1107COOH- MSNNH2. Amine ended mesoporous silica nanoparticles and carboxyl ended Tetronic T1107 copolymers are attached as shown in Figure 4.16.

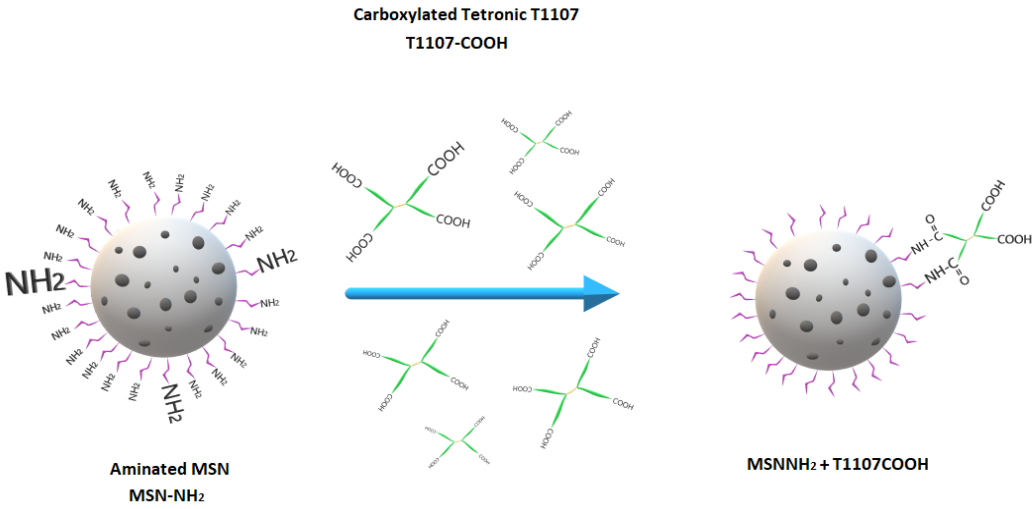

Figure 4.16. Schematic of synthesis of $MSNNH_2$-T1107COOH.

Attachment of aminated Pluronic/Tetronic to carboxylated MSN (or carboxylated MSN to aminated Pluronic/Tetronic) is achieved by click chemistry. In chemical synthesis, click chemistry generates substances quickly and reliably by joining small units together.

Click chemistry is not a single specific reaction, but describes a way of generating products by following the examples in nature, which also generates substances by joining small modular units.

By using click chemistry, $MSNNH_2$ (or MSNCOOH) is covalently attached with T1107COOH (or $T1107NH_2$), which serve as a gate against releasing the cargo inside the $MSNNH_2$ unless desired.

Bare $MSNNH_2$ or any other MSN type tend to release cargo as soon as they are introduced into aqueous media. However, here, clicked T1107COOH keeps the drug inside the pores of $MSNNH_2$. Since T1107COOH is pH and temperature sensitive, the gate opens only at specific temperature and pH conditions which prevents premature release of cargo until the targeted cell.

At this point, it is important to select the correct ratio of amounts between copolymer and nanoparticles. At first, for MSNCOOH-$T1107NH_2$ and $MSNNH_2$-T1107COOH, 1.45 g copolymer is used for 80 mg nanoparticle. For MSNCOOH-$F127NH_2$, 0.8 g copolymer is used for 80 mg nanoparticle.

It is observed that, if the copolymer amount is less than it is supposed to be, the pores remain open and the gating mechanism cannot work as desired. Likewise, if copolymer amount is more than it is expected, all pores are completely covered with the copolymer and the cargo release will be difficult.

After release experiments and FTIR results, these ratios are adjusted until optimum ratio is found which is 2.1 g copolymer and 100 mg nanoparticle for $MSNNH_2$-T1107COOH, 1 g copolymer and 100 mg nanoparticle for MSNCOOH-$T1107NH_2$ and 0.77 g copolymer and 100 mg nanoparticle for MSNCOOH-$F127NH_2$.

Moreover, during the click chemistry, sonication is applied to separate the nanoparticles from each other. Otherwise two or more nanoparticles can be conjugated and functionalized together.

Figure 4.17 shows the STEM images of T1107COOH capped $MSNNH_2$ nanoparticles after covalent bonding. Due to drying process for STEM analysis, nanoparticles are observed to stick to each other. There is no significant size variation between $MSNNH_2$ and $MSNNH_2$-T1107COOH.

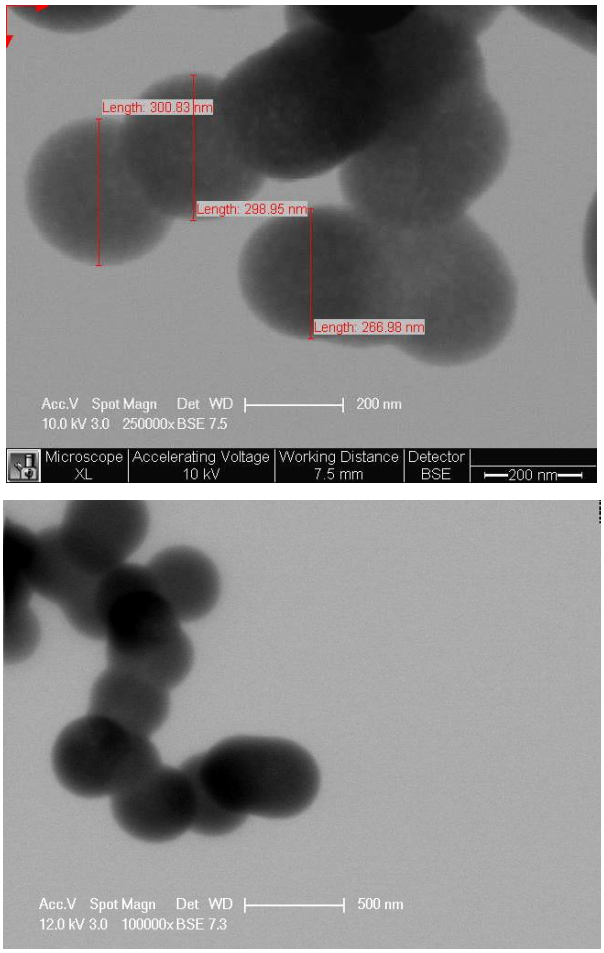

Figure 4.17. STEM images of $MSNNH_2$-T1107COOH.

In Figure 4.18, FTIR results from covalent bonding of T1107COOH-$MSNNH_2$ is illustrated. Between 1500-1700 cm^{-1} range, amide formation is confirmed by the presence of two peaks.

Also, it can be seen the peak at 1750 cm^{-1}, which corresponds to carbonyl stretching vibration for T1107COOH, has disappeared. This phenomenon is caused by the removal of carbonyl group from the material which is transformed into amide structure. Also as shown in Table 4.1 and Figure A.5, zeta potential value for $MSNNH_2$-T1107COOH is +13.43.

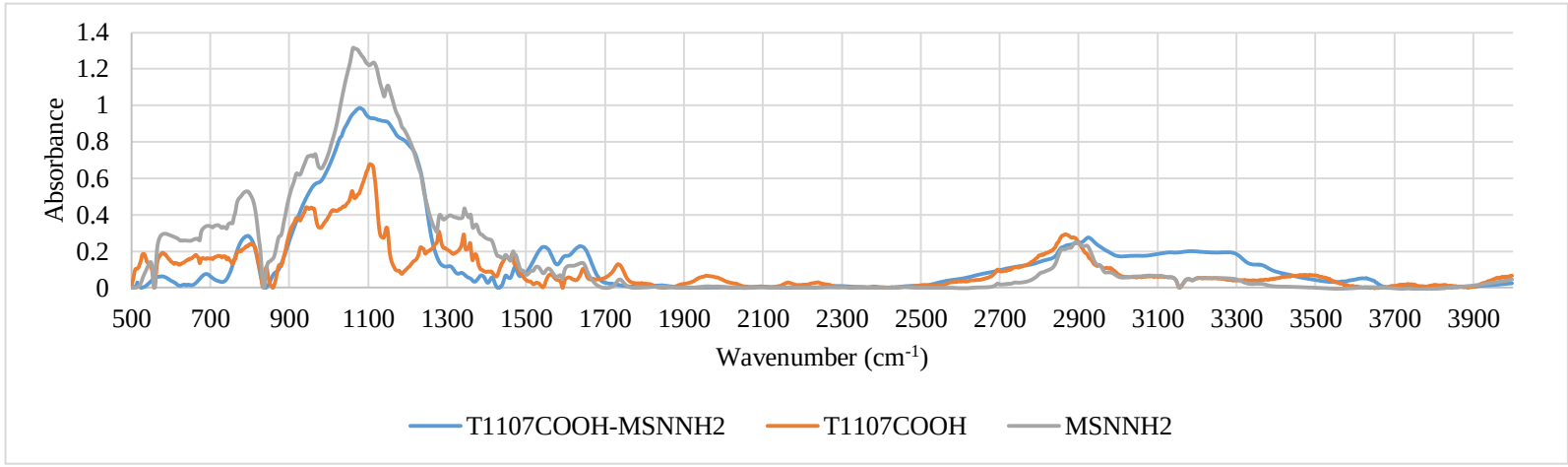

Figure 4.18. FTIR spectra of T1107COOH, $MSNNH_2$ and T1107COOH-$MSNNH_2$.

In order to understand gating mechanism efficiency, diffusion experiments are performed. However, here, curcumin is not used, but arginine is preferred as cargo molecule due to its hydrophilic nature. As explained in Section 4.1.2.1 and 4.1.2.2, cargo release experiments are conducted at different temperature and pH values.

As it is illustrated in Figure 4.19, T1107COOH-MSNNH2 releases its cargo most at 43℃ and pH 7.4. This can be explained by the temperature sensitive nature of T1107COOH. Even after the synthesis process, the material needed to be kept in cold environment. Otherwise, it starts to melt in room temperature. In this case, the highest cargo release rate observed at 43℃ and pH 7.4 is probably due to the break down of the gating mechanism. However, this temperature (43℃) is used to investigate the behaviour of materials at higher temperatures.

As expected, at 37℃ and pH 4.8 cargo release is relatively high compared to those at the other conditions. On the other hand, at 25℃ and pH 7.4, arginine release rate is minimum. Hence, this material can be stored in cold environment until it is introduced into to the body. Moreover, as shown in Figure 4.19, T1107COOH gated MSNs would release the cargo most in the acidic environment which can be considered for cancer treatment.

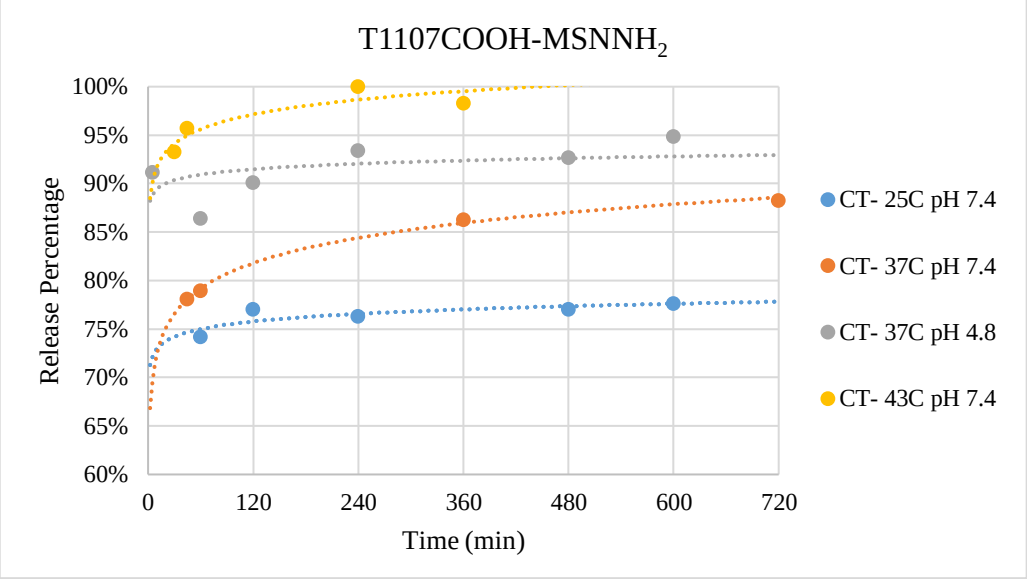

Figure 4.19. Release of arginine from T1107COOH-MSNNH$_2$.

4.2.2. Aminated Tetronic T1107 gated Carboxylated MSNs (T1107NH_2-MSNCOOH)

4.2.2.1. Synthesis and Characterization of Carboxylated MSN (MSNCOOH). Carboxyl ended mesoporous silica nanoparticles are produced by using amine functionalized mesoporous silica nanoparticles exposed to ring opening reaction of succinic anhydride as illustrated in Figure 4.20.

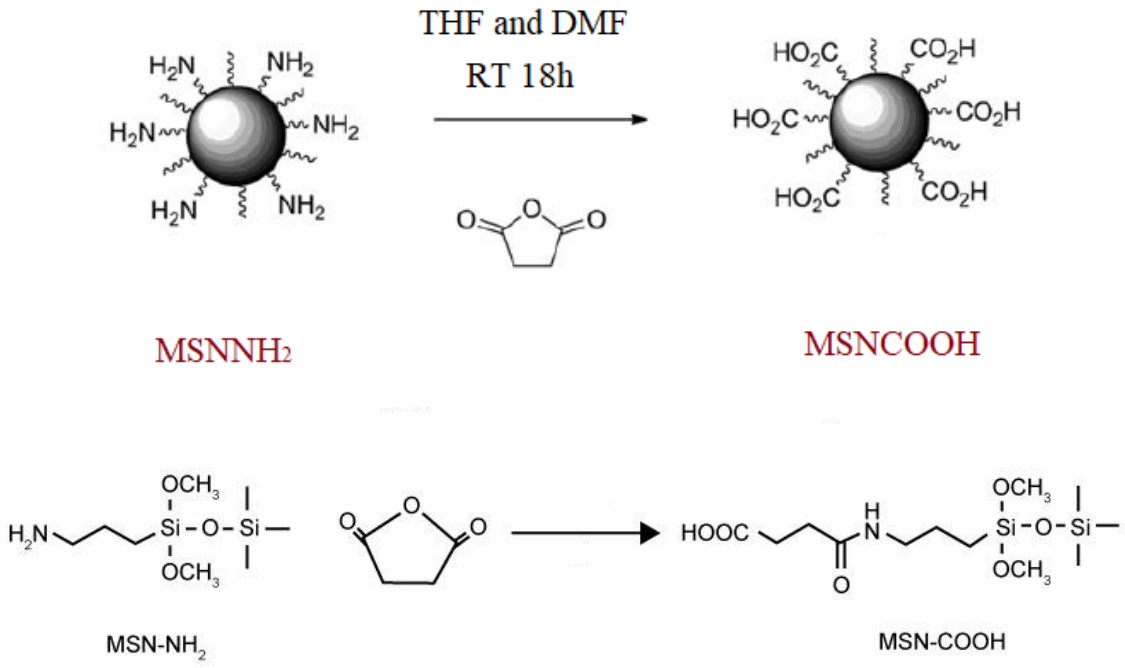

Figure 4.20. Schematic of carboxylation process for MSN.

In order to adjust carboxylated mesoporous silica nanoparticle size, first amine ended nanoparticles should be produced carefully. For amine ended nanoparticle synthesis, in the very beginning of the reaction, CTAB should be added to the reaction mixture as template. However, the time length of CTAB addition is not mentioned in the protocol given by Kim *et al*., (2012). It is observed that duration of CTAB addition affects the nanoparticle size.In this study CTAB is added into the solution in 2.5 hours. STEM results indicate a particle diameter of

approximately 230 nm as shown in Figure 4.21. Sonication during synthesis is very important which can result in more uniform shape and size distributions.

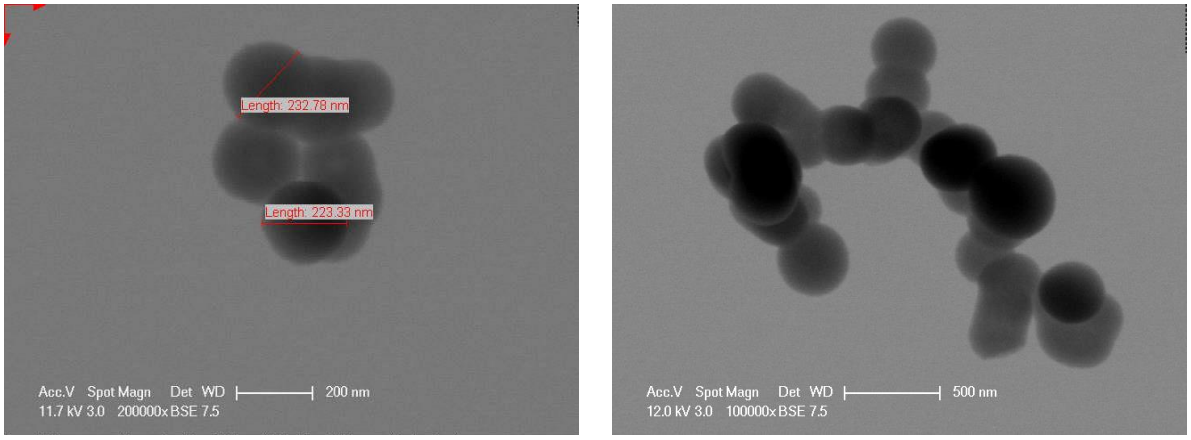

Figure 4.21. STEM images of MSNCOOH.

According to Feifel *et al.*, (2011), carboxyl peaks of carboxylated mesoporous silica nanoparticles are at 1725 cm^{-1} and 1461 cm^{-1}, Si-O-Si asymmetric stretching vibration occurs between 1020-1110 cm^{-1} and Si-OH asymmetric bending and stretching vibration appears at 960 cm^{-1}.

In Figure 4.22, occurrence of carboxyl peaks are verified by the peaks at 1650 cm^{-1} and 1410 cm^{-1}. Si-O-Si asymmetric stretching vibration is verified by the peak at 1060 cm^{-1} and Si-OH asymmetric bending and stretching vibrations are verified by the peak at 960 cm^{-1}. As demonstrated in Table 4.1 and Figure A.4, carboxylated mesoporous silica nanoparticles are negatively charged with a zeta potential value of -17.42.

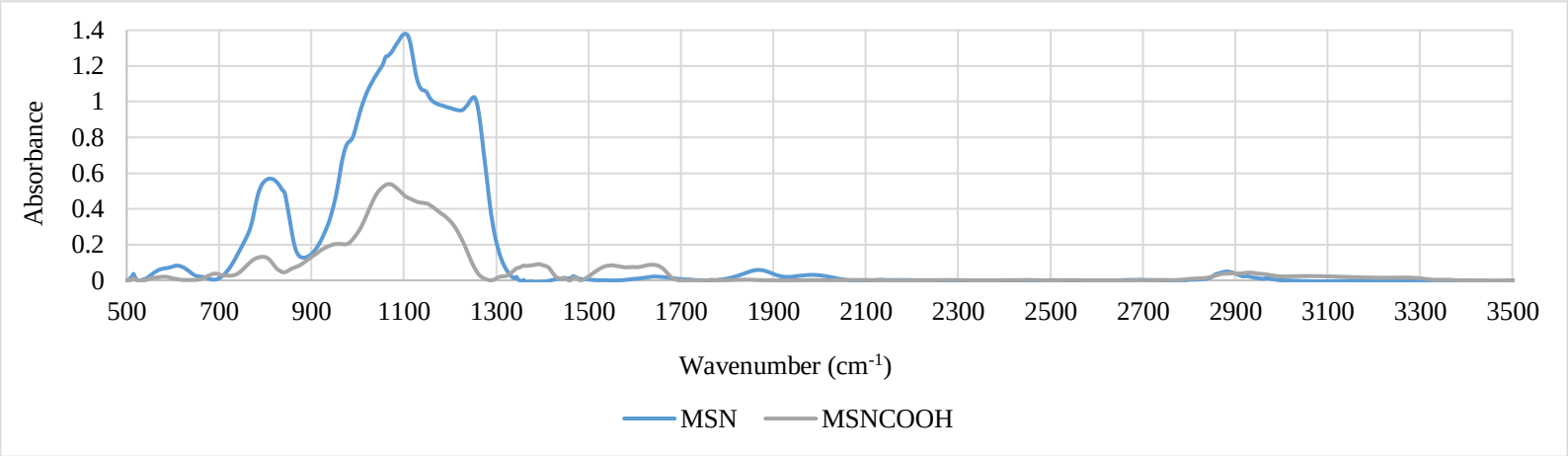

Figure 4.22. FTIR spectra of MSN and MSNCOOH.

4.2.2.2. Synthesis and Characterization of Aminated Tetronic T1107 (T1107NH_2). Synthesis of amine ended Tetronic T1107 is achieved by slight modification of the method reported by Zhang *et al*., (2011) for amination of Pluronic F127.

In order to prepare aminated Tetronic T1107 (or Pluronic F127), first, terminal –OH groups of Tetronic T1107 (or Pluronic F127) is activated with CDI. Tetronics are X shaped copolymers which have four –OH ended arms. Hence, CDI activation is applied through all –OH ends as shown in Figure 4.22.

While activating the Tetronic T1107 with CDI, the amount of CDI is very crucial. If there is no sufficient amount of CDI in the reaction mixture, some –OH groups cannot be activated and remain as they are. Once in the same reaction mixture, CDI activated Tetronic ends and non CDI activated –OH ends of Tetronic crosslink with each other.

Consequently, transparent, very hard and flexible gels are obtained at the end of the reaction, preventing the second step of the amination method to be followed. To avoid this situation, CDI amount in the reaction should be in excess by at least 79.8X of molar Tetronic amount.

Moreover, CDI activated Tetronic T1107 copolymers can easily become a gel in contact with air and above 25℃. Moisture in the air can easily effect the condition of the end product which may result in failure of further steps of the reaction.

Hence storage conditions are very important, as in the gel form, it is hard to define the exact amount of the material. So, for further steps it is very hard to measure its weight, therefore molar ratios can not be adjusted as it is supposed to be. Hence, this product should be kept in cold and dry conditions.

Pluronic F127, white power is obtained at the end of the reaction and these problems are not observed.

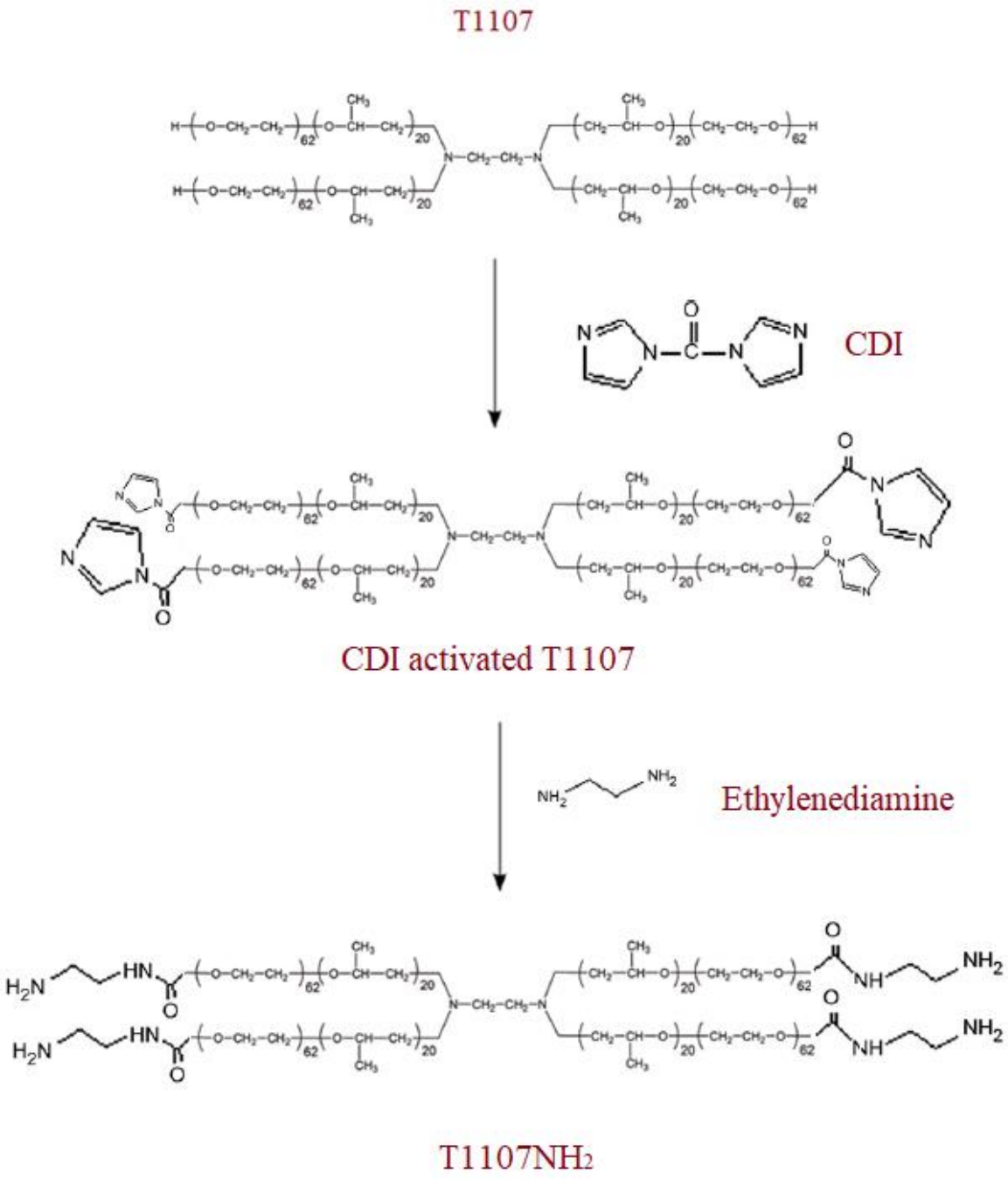

Figure 4.23. Schematic of amination process for Tetronic T1107.

In the second step of amination, CDI activated ends of T1107 are changed with amine ends by using ethylenediamine as illustrated in Figure 4.23. In the synthesis, the solvent (anhydrous acetonitrile) volume play a critical role. If acetonitrile volume is not enough, it is

very hard to extract aminated Tetronic T1107 at the end of the reaction. In the protocol given by Zhang *et al.*, (2011), excess amount of ethylenediamine is removed by a rotary evaporator then the remaining product is precipitated in ether and again the remaining ethylenediamine is removed as dissolved in ether. However, with Tetronic, ether cannot be removed by a rotary evaporator since aminated Tetronic T1107 remains in the liquid form after extraction of ether. Instead, the product is precipitated in cold ether, then ether and ethylenediamine dissolved in ether are removed easily by liquid separator glass funnel. Then, the product is dried under vacuum immediately to avoid gel formation.

FTIR analysis is performed to verify the functionalization of T1107. For amine-ended Tetronic T1107, a peak for carbonyl group appears at 1720 cm^{-1}, as reported by Zhang *et al.*, (2011). Also, two peaks (similar to camel hump shape) are observed between 1500-1700 cm^{-1} which are caused by amide formation in $T1107NH_2$ as shown in Figure 4.24. Moreover, a peak occurs between 2120-2145 range for $T1107NH_2$ which corresponds to carbodiimide structure. In other words, unreacted CDI still remains on the T1107.

4.2.2.3. Synthesis and Characterization of $T1107NH_2$-MSNCOOH. As demonstrated in Figure 4.25, carboxylated mesoporous silica nanoparticles and aminated Tetronic T1107 are attached using EDAC.

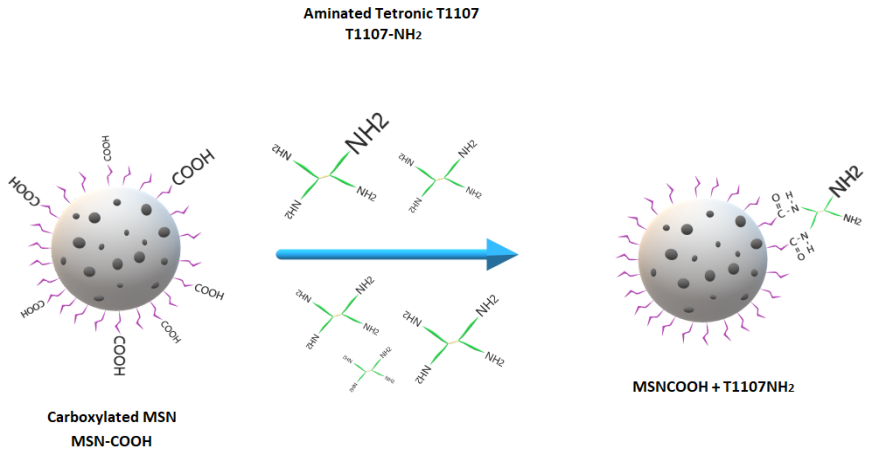

Figure 4.24. Schematic of synthesis of MSNCOOH and $T1107NH_2$.

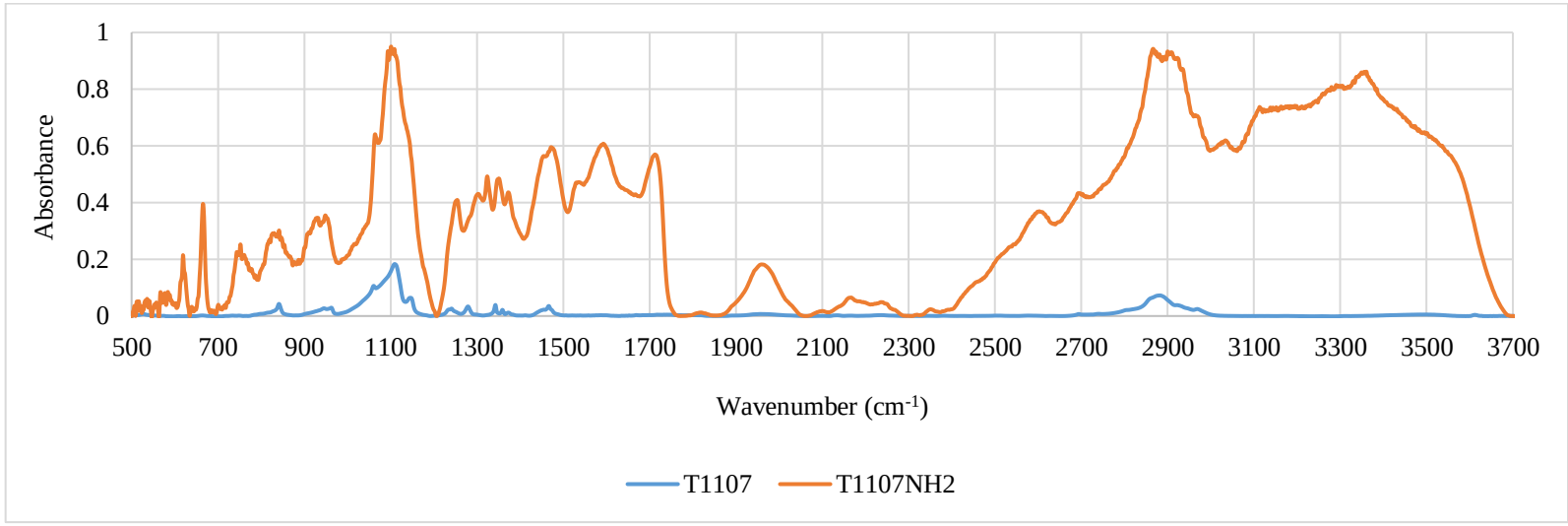

Figure 4.25. FTIR spectra of aminated Tetronic T1107 and T1107NH_2.

Attachment of aminated Tetronic T1107 to carboxylated MSN is achieved by click chemistry as described in Section 4.2.1. By using click chemistry, surfaces of MSNCOOH is modified with $T1107NH_2$ which serve as a gate. Sonication is used in order to prevent aggregation of particles.

In Figure 4.26, STEM images of $T1107NH_2$-MSNCOOH particles are given which are roughly between 290-340 nm. A small amount of size variation is observed between $T1107NH_2$-MSNCOOH and bare MSNCOOH (230 nm) due to the presence of copolymer.

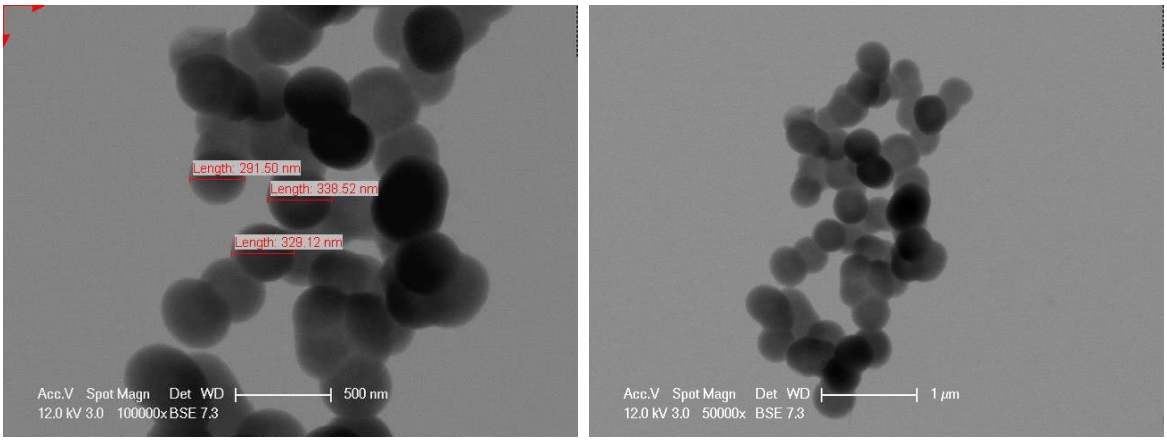

Figure 4.26. STEM images of MSNCOOH-$T1107NH_2$.

The click chemistry using EDAC results in amide formation between particles and copolymer which can be detected by FTIR analysis. In Figure 4.27, related IR spectra of amine ended-tetronic gated MSNs is given. For amine ended Tetronic gated MSNs, amide formation due to covalent bonding between aminated Tetronic T1107 (T1107NH2) and carboxylated mesoporous silica nanoparticles (MSNCOOH) can be seen between 1500-1700 cm^{-1} as two peaks. Also, around 1400 cm^{-1} a decrease in peak intensity is observed corresponding to the vanishing of O-H bending of carboxylic acid. Moreover, a zeta potential value of -25.76 is measured for $T1107NH_2$-MSNCOOH, as demonstrated in Table 4.1 and Figure A.6.

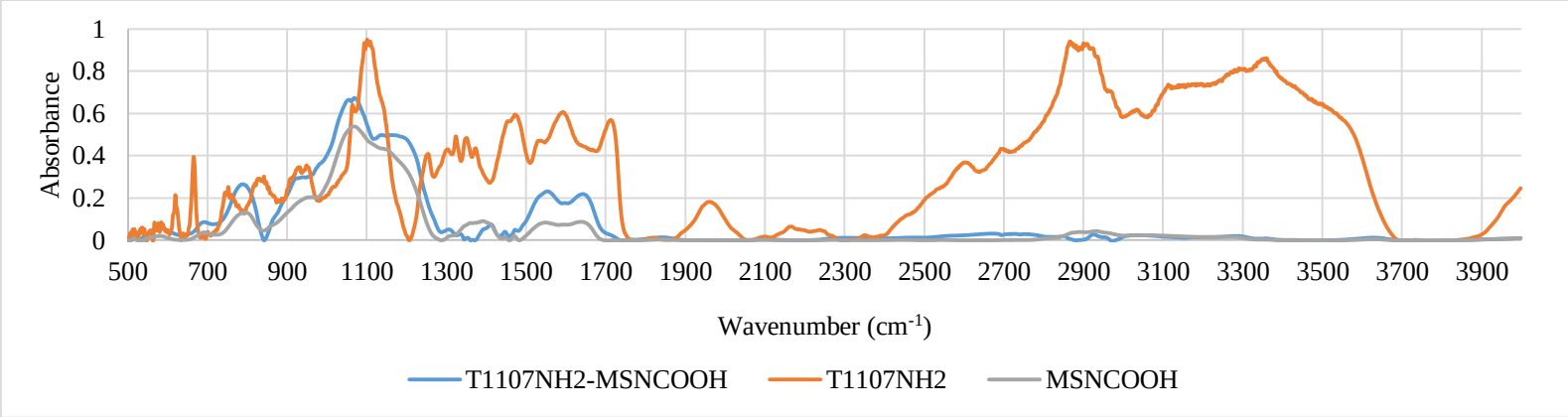

Figure 4. 27.FTIR Results of clicked $T1107NH_2$ and MSNCOOH ($T1107NH_2$-MSNCOOH).

As it can be seen in Figure 4.28, the gating mechanism works best in acidic environment at low temperatures. According to De Lisi *et al*., (2011), as temperature and pH decreases, Tetronic T1107 tends to release the cargo more. In accordance with that observation, there is minimal cargo release at temperatures 37 ℃ and 43℃ at pH 7.4.

Moreover, the release is maximum at 37 ℃ and pH 4.8 followed by the one at 25 ℃ and pH 7.4. Hence, with T1107NH2-MSNCOOH, drug loaded mesoporous silica nanoparticles will keep most of the cargo inside the pores until they meet acidic cell environment like cancer cells.

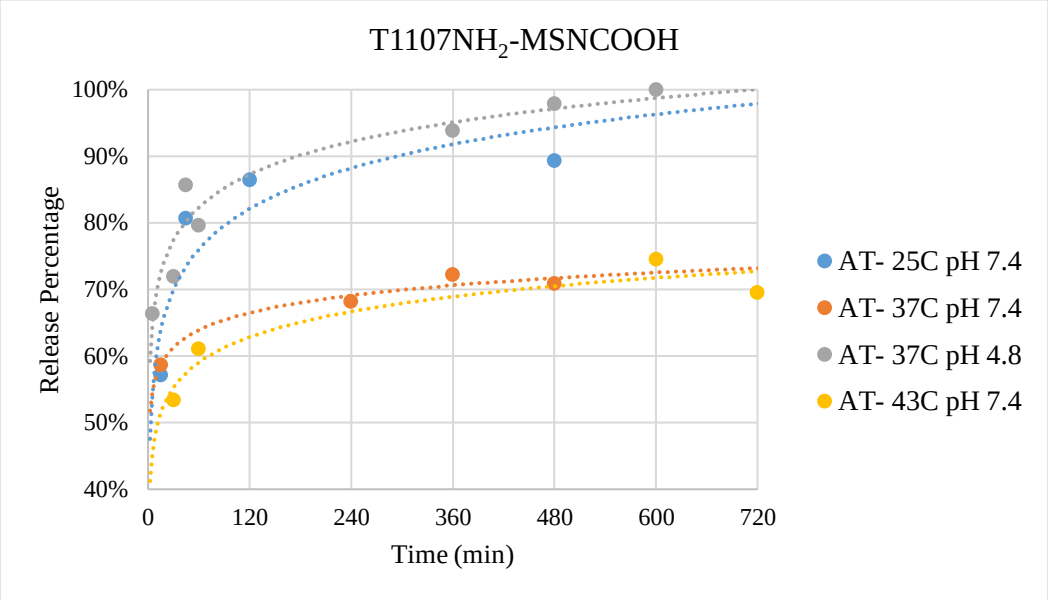

Figure 4.28. Release of arginine from T1107NH_2-MSNCOOH.

4.2.3. Aminated Pluronic F127gated Carboxylated MSNs (F127NH_2-MSNCOOH)

4.2.3.1. Synthesis and Characterization of Carboxylated MSN (MSNCOOH). Synthesis and characterization of MSNCOOH is described in Section 4.2.2.1.

4.2.3.2. Synthesis and Characterization of Aminated Pluronic F127 ($F127NH_2$). Amination of Pluronic F127 is achieved by the same protocol reported by Zhang *et al*., (2011). The chemistry behind this reaction is the same as described in Section 4.2.2.2. First, -OH end of the Pluronic F127 is activated with CDI, then activated ends are functionalized with ethylenediamine as illustrated in Figure 4.29.

Again, the amount of CDI, solvent and ethylenediamine is very important. However, in the protocol, amounts are given very clearly and hence amination of Pluronic F127 is perfomed without any obstacle. In general, amination of Pluronic F127 is easier compared to amination of Tetronic T1107 because there is less risk of crosslinking –OH ends with activated ends after activation.

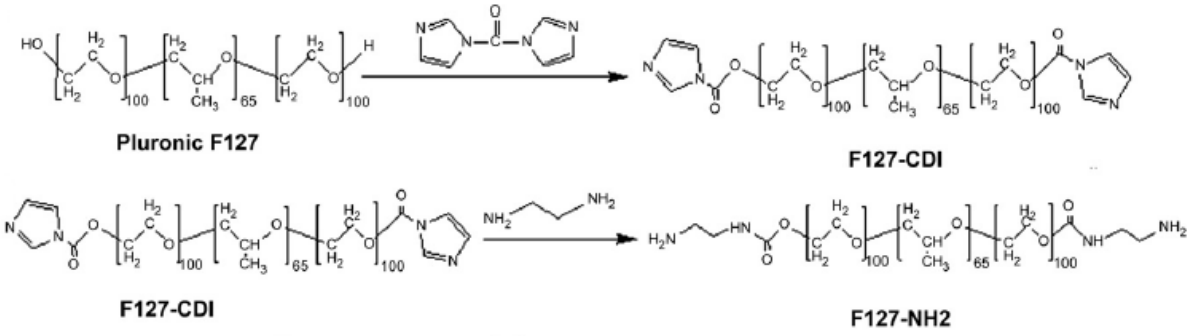

Figure 4.29. Schematic of amination process for Pluronic F127 [47].

Functionalization of Pluronic F127 is verified by FTIR analysis. As mentioned before, carbonyl group peak occurs at 1720 cm^{-1} according to the literature. In Figure 4.30, a peak is observed at 1720 cm^{-1} demonstrating successful functionalization of Pluronic F127. Moreover, a zeta potential value of as -12.20 is measured for $F127NH_2$-MSNCOOH as illustrated in Table 4.1 and Figure A.7.

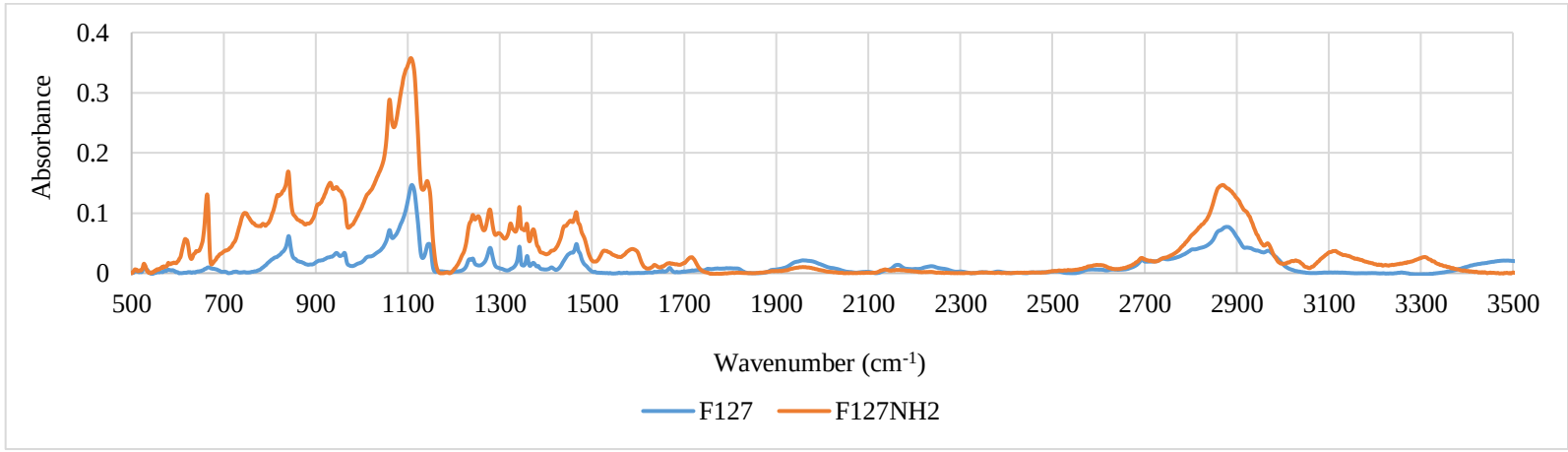

Figure 4.30. FTIR spectra of F127 and F127NH_2.

4.2.3.3. Synthesis and Characterization of F127NH2-MSNCOOH. Click chemistry between carboxylated mesoporous silica nanoparticles (MSNCOOH) and aminated Pluronic F127 ($F127NH_2$) is demonstrated in Figure 4.31. For gating of MSNCOOH with $F127NH_2$, the protocol given by Zhang *et al.*, (2011) is followed.

Arginine is used as cargo as well and the same conditions are applied to examine temperature and pH response of F127NH2 gated MSNCOOHs.

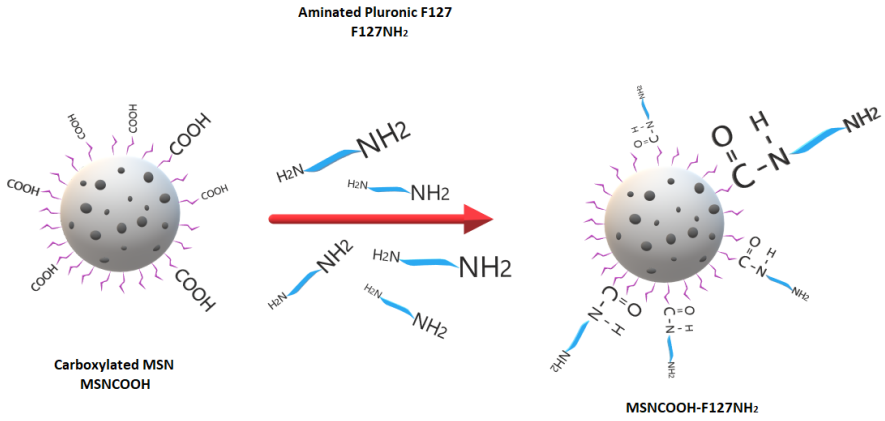

Figure 4.31. Schematic of synthesis of MSNCOOH and $F127NH_2$.

As mentioned before, the particle size of MSNCOOH has roughly been found around 230 nm by STEM analysis. In Figure 4.32, STEM results for - $F127NH_2$ gated MSNCOOH are shown. Particle diameter of MSNCOOH-$F127NH_2$ is approximately 280-340 nm. Hence, slight size variation is recorded by STEM after gating the NPs.

Similar to the cases reported with functionalized T1107, $F127NH_2$ sticks to the MSNCOOH surface after getting dried for STEM analysis which gives comparable particle sizes for MSNCOOH and MSNCOOH-$F127NH_2$.

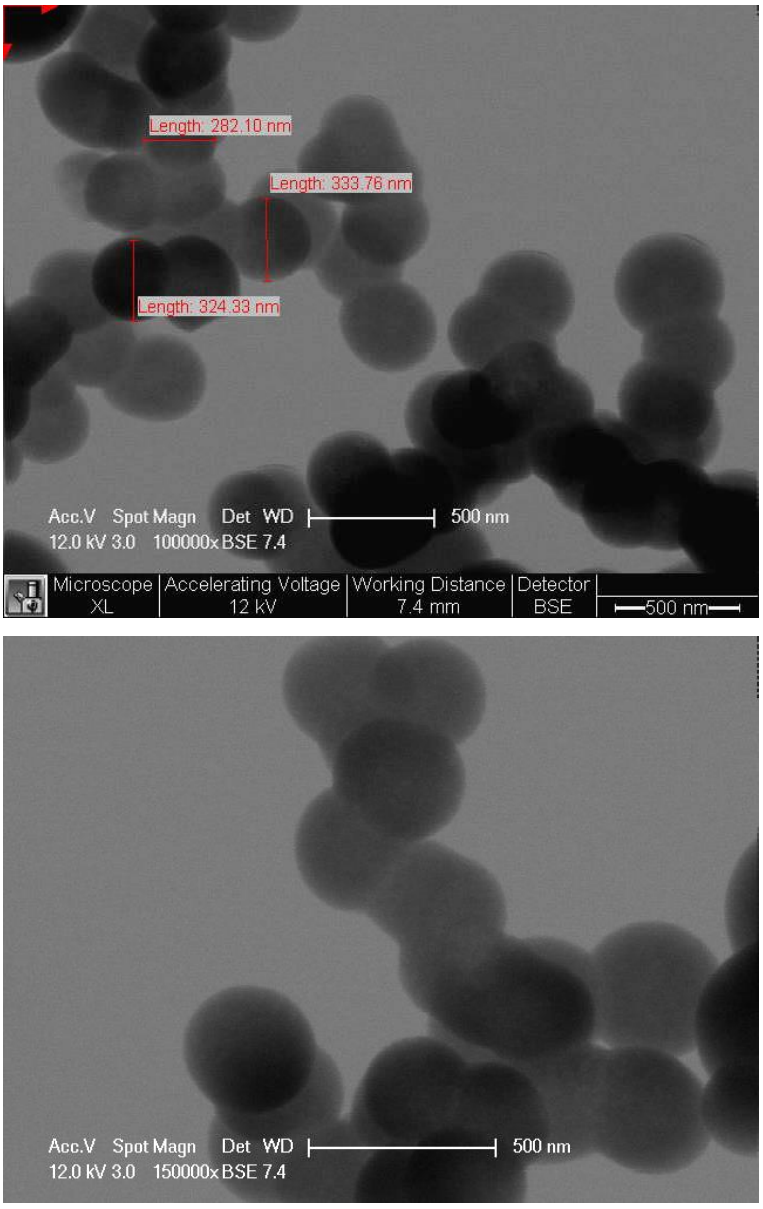

Figure 4.32. STEM images of F127NH2-MSNCOOH.

In Figure 4.33, IR spectra for MSNCOOH-F127NH_2 is given. Amide formation can be observed clearly between 1500-1700 cm^{-1} as two peaks in camel hump shapesuggesting that click chemistry is achieved for MSNCOOH and F127NH_2.

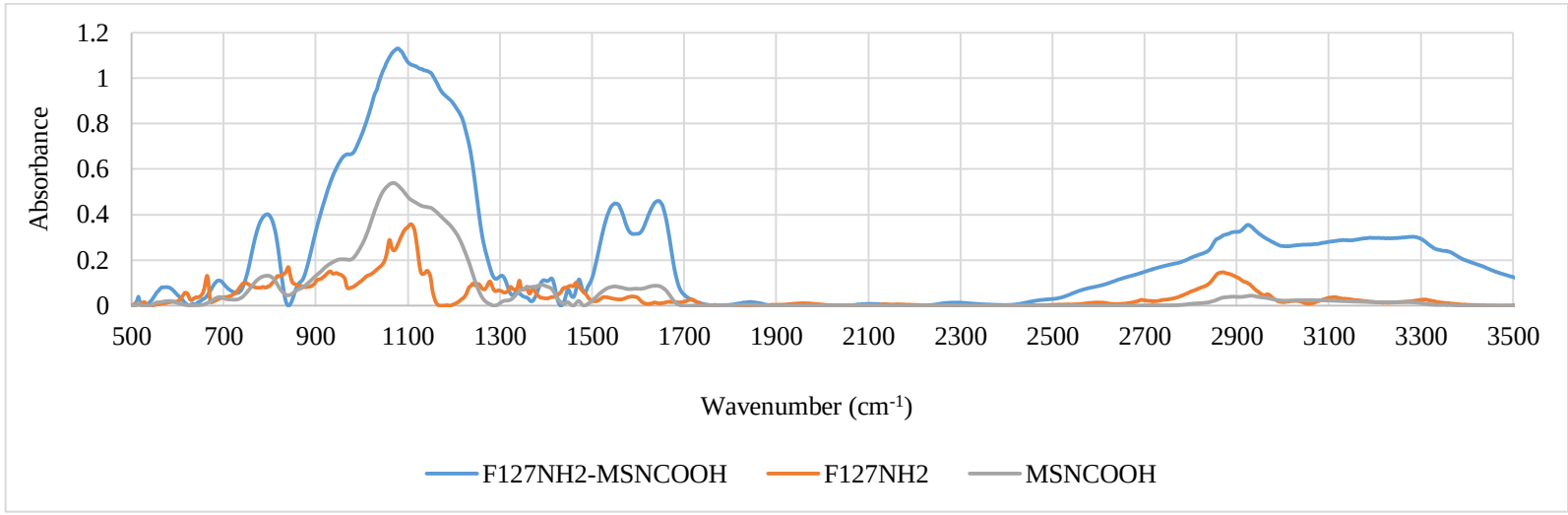

Figure 4.33. FTIR spectra of MSNCOOH, F127NH_2, and MSNCOOH-F127NH_2.

In Figure 4.34, release data of arginine through MSNCOOH-F127NH_2 is illustrated. According to the graph, there is minimum release at 37 ℃ and pH 4.8, as Pluronic F127 tends to release the cargo most efficiently at high pH value. At 37 ℃ and pH 7.4 as well as 43 ℃ and pH 7.4, the release rate is considerably large. At 25℃ and pH 7.4 cargo release is maximum in agreement with the findings of Basak *et al*., (2013), which indicate Pluronic F127 micelles tend to release the cargo more at low temperatures and high pH values.

In addition, Pluronic F127 (53-57 ℃) has higher melting point than Tetronic T1107 (~50℃), hence the gating mechanism using Pluronic F127 is stronger against higher temperatures. Therefore, at 43℃, aminated Pluronic (F127NH_2) gates are probably not corrupted.

According to research conducted by Gentile *et al*., (2010), F127 tends to self assemble into a macromolecule with increasing temperature at high concentration. According to the article, this phenomenon is related with the strength of interaction between the rheological units (PEO and PPO units).

Therefore, taking into consideration the parameters given as well as the temperature values for release experiments in this research, the most interaction between the copolymer units is expected to occur at 37℃, then at 43℃, followed by 25℃. In agreement with this finding, in Figure 4.34, MSNCOOH-F127NH_2 (AF) tend to release arginine most at 25℃ due to weak interaction between polymer units. This phenomenon is also confirmed by the research made by Basak *et al*., (2013).

The least release for Pluronic F127 is observed at 37℃ and pH 4.8. In other words, as the interaction gets stronger between the units, the chains shrink closing the pores, and hence the cargo release rate decreases.

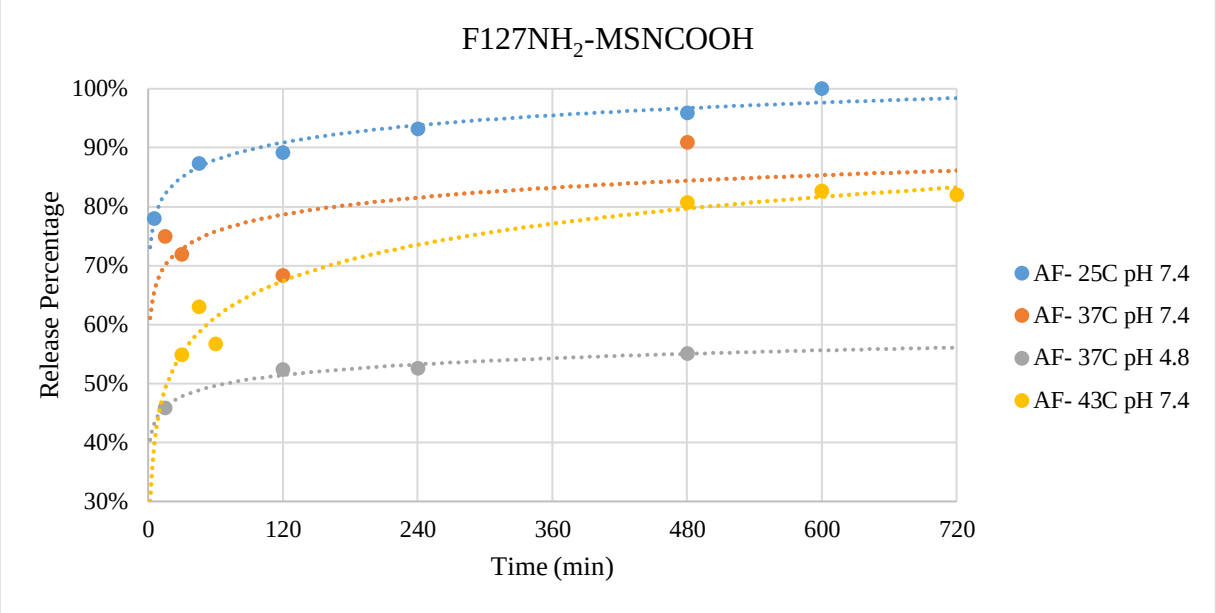

Figure 4.34. Release of arginine from F127NH_2-MSNCOOH.

4.2.4. Comparison of Pluronic and Tetronic Gated MSNs

As illustrated in Figure 4.35, the highest release rate is observed for MSNCOOH-T1107NH_2 (AT) at 37℃ and pH 4.8. At 25℃ and pH 7.4 the release rate is still high for MSNCOOH-T1107NH_2 which is consistent with the findings of De Lisi *et al*., (2011).

De Lisi *et al*. suggest that there is inverse effect of temperature on the release rate of T1107, i.e, as temperature increases, release rate for T1107 decreases. However, apparently this is not the case for MSNNH_2 -T1107COOH (CT).

According to Figure 4.35, lowest release rate is for MSNCOOH-F127NH_2 at 37℃ and pH 4.8, which indicates that MSNCOOH-F127NH_2 is not an effective mechanism in manner of pH responsiveness.

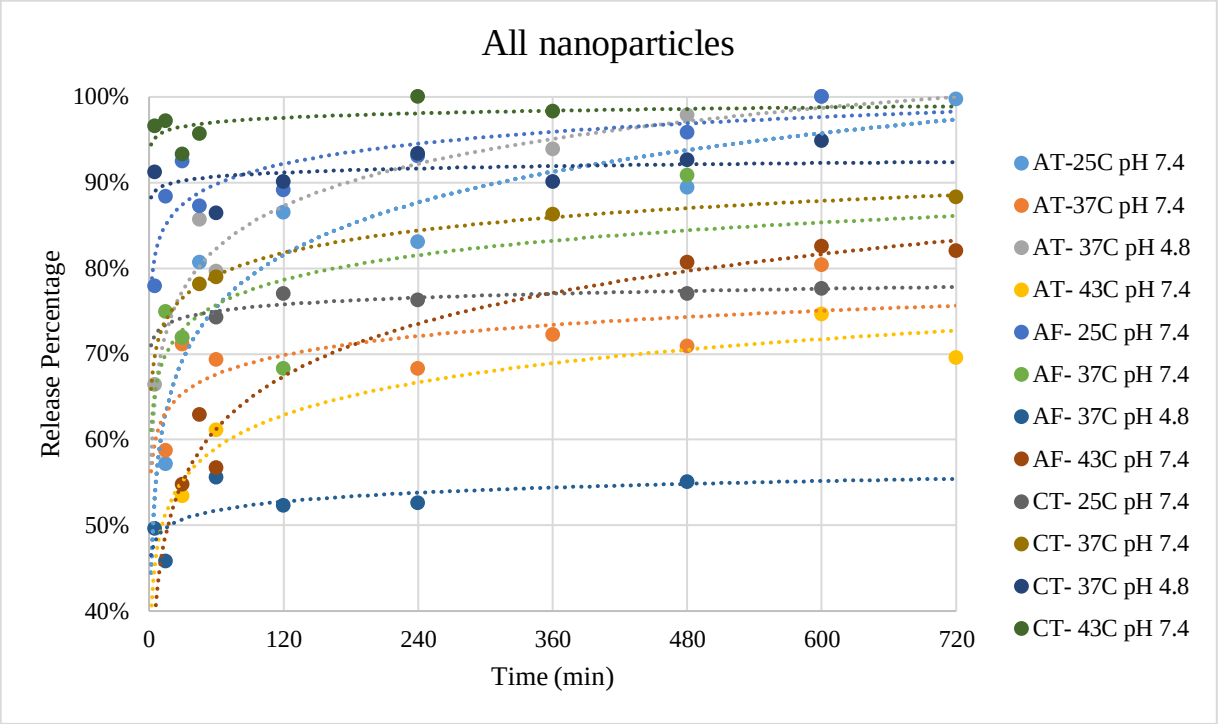

Figure 4.35. Release of arginine for MSNNH2-T1107COOH, MSNCOOH-T1107NH2 and MSNCOOH-F127NH$_2$.

According to Kim *et al.*, (2012), amination of MSN provides positive charge to the pore surface which is confirmed with zeta potential measurements as illustrated in Table 4.1. In Table 4.1 it is also demonstrated that the diameter of the MSNNH$_2$ and MSNCOOH nanoparticles slightly increase upon gating.

Table 4.1. Table of STEM and Zeta Potential Results.

	STEM (nm)	**Zeta Potential (mV)**
MSNNH$_2$	120-200	+39.90
MSNCOOH	230	-17.42
MSNNH$_2$-T1107COOH	260-300	+13.43
MSNCOOH-T1107NH$_2$	230	-25.76
MSNCOOH-F127NH$_2$	280-340	-12.20

4.3. Cargo Loading Experiments

To understand the loading capacity of nanoparticles UV-Vis experiments are performed. In the physical attachment method, hydrophobic mesoporous silica nanoparticles are soaked into 10 mg/ml curcumin solution before the gate formation. Then the solution is removed and curcumin loaded nanoparticles are dried. 50 mg of curcumin loaded, dried hydrophobic mesoporous silica nanoparticles are then introduced into the hot water (approximately 90 ℃) and stirred for 1 hour. Visible amount of the curcumin particles are unloaded and diffused into water. This solution gives an absorbance value of 1.505 in the UV-Vis spectroscopy measuements, which corresponds to 80 µg/mL curcumin solution. In other words, 0.8 % of the 10 mg/ml curcumin solution is entered into the hydrophobic mesoporous silica nanoparticle pores.

With the chemical method, arginine loading is done after the gate is constructed. In the same way, 10 mg/ml of arginine water solution is used and analyzed in UV-Vis spectroscopy. After the completion of loading process, nanoparticles are removed from the solution, then residual solution is collected and analyzed by UV-Vis spectroscopy. The difference between the absorbance values of 10 mg/ml arginine solution and the residual solution is investigated. As illustrated in Table 4.2, there is no significant difference in percentage values for different gate types, but, MSNCOOH-T1107NH2 is slightly more effective in loading the cargo to the pores.

Table 4.2. Cargo Loading Percentage Values.

	Absorbance	**Cargo Loading Percentage**
10 mg/ml Arginine + Water Solution	3.269	-
MSNNH2-T1107COOH	3.152	3.6%
MSNCOOH-T1107NH2	3.140	4.1%
MSNCOOH-F127NH2	3.180	2.8%

4.4. Toxicity Analysis

Toxicity of synthsized particles is investigated using *saccharomyces cerevisiae* as model cells and performing CFU analysis. The cells are exposed to the particle concentrations two different particle concentrations 250 µg/L and 500 µg/L. As illustrated in Figure 4.36 and Table 4.3, nanoparticles produced by physical attachment method are highly toxic compared to those produced by chemical attachment method. In the physical attachment method, the average nanoparticle diameter is approximately between 80-100 nm. Smaller nanoparticles can easily penetrate the cell and they may accumulate more within the cell [49]. Hence, smaller nanoparticles may be more toxic than larger nanoparticles. Moreover, the physically attached gates may not be as durable as chemically attached gates. The break down of the gates results in bare hMSNs, which could be highly toxic due the hydrophobic nature of the particle.

Considering different types of the gates produced by chemical attachment method, aminated pluronic and carboxylated tetronic are observed to perform better than aminated tetronic in terms of cell viability, as demonstrated in Figure 4.36. This is attributed to biocompatible carboxylated tetronic nature, according to Park *et al.*, (2010) carboxylated tetronic has no apparent cytotoxicity and has a great potential for drug delivery systems and tissue engineering.

Table 4.3. CFU analysis for nanoparticles.

	Charge	**250 µg/L**	**500 µg/L**
MSNNH$_2$ + T1107COOH	+	67.24	87.07
MSNCOOH + T1107NH$_2$	-	59.48	24.14
MSNCOOH + F127NH$_2$	-	82.76	69.83
T1107 (Physical Attachment)		19.83	5.17
F127 (Physical Attachment)		13.79	8.62

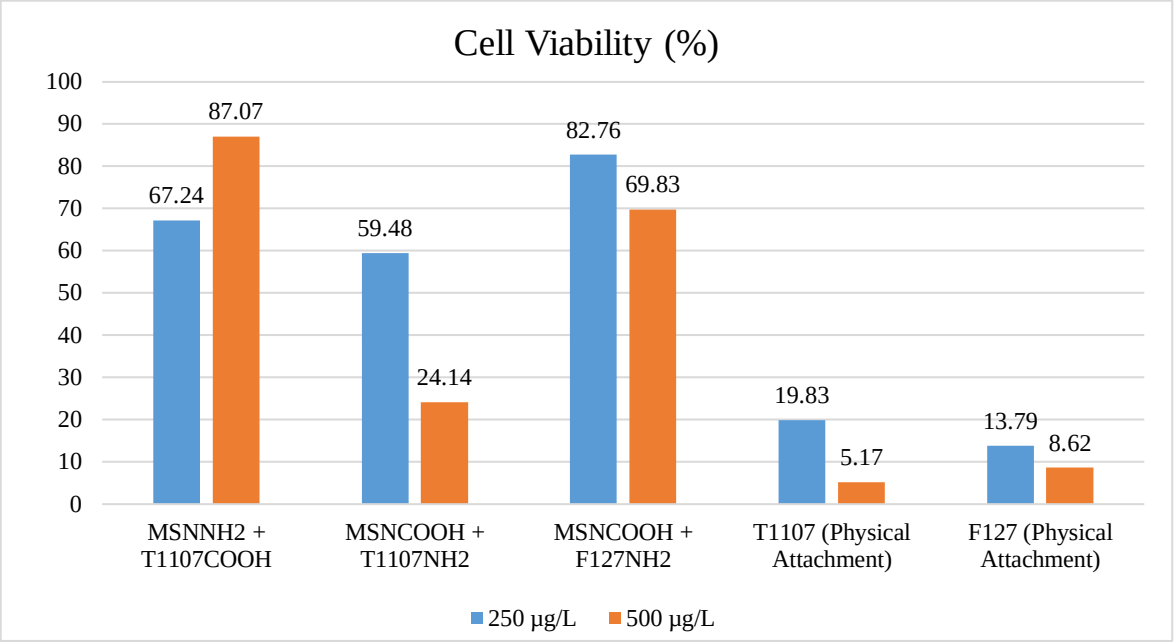

Figure 4.36. Viability percentage for all types of nanoparticles.

5. CONCLUSION

The aim of this work is to investigate the gating efficiency of Tetronic capped mesoporous silica nanoparticles for drug delivery purposes. Pluronics, the widely studied counterparts of Tetronics, are also used to compare the results. Two different approaches, i.e., physical gating and chemical gating, are used to construct the gates over MSNs. For this purpose, different types of MCM-41 are produced as drug carriers.

In the physical gating approach, surfaces of MSNs are modified with octyl groups to form a hydrophobic layer. Bare MSNs are also produced as a control group. While hMSNs are observed to float on the water, bare MSNs sink to the bottom of the water container, suggesting succesful surface modification with octyl groups. STEM/SEM analysis are performed for further characterization of nanoparticles. The average diameter of nanoparticles are found to be roughly 50-60 nm for bare MSNs and 80 nm for octyl modified MSNs. Then, by taking the advantage of hydrophobic/hydrophilic nature of Tetronics/Pluronics, physical attachment is achieved between hydrophobic surface of hMSN and hydrophobic PPO units of the copolymer. While PPO units of Pluronics/Tetronics are adsorbed to the hydrophobic surface of hMSN, hydrophilic PEO units of the copolymer are repelled by the hydrophobic surface of hMSNs and attracted by the aqueous media. Therefore, physically gated hMSNs can disperse in water while bare hMSNs cannot. In this study, Pluronics F127 and Tetronics T1107 are selected for their wide use in pharmaceutics cosmetics. After gating hMSNs by physical means, STEM and DLS analysis are performed, yielding in the average particle diameters of 100 nm and 718 nm for F127-hMSNs, as well as 80 nm and 306 nm for T1107-hMSNs, respectively. Next cargo loading and release experiments are performed to understand the efficiency of the gating mechanism. In the this approach, curcumin is used as drug/cargo molecule due to its hydrophobic nature, which is compatible with hMSNs. Four different temperature and pH conditions are used in the experiments which are 25℃ and pH 7.4, 37℃ and pH 4.8, 37℃ and pH 7.4 as well as 43℃ and pH 7.4. With F127, the release of curcumin is found to be the most at 43℃ and pH 7.4 followed by 37℃ and pH 4.8, 37℃ and pH 7.4, 25℃ and pH 7.4. With T1107, curcumin release

is the most at 37℃ and pH 4.8, followed by 43℃ and pH 7.4, 37℃ and pH 7.4, and 25℃ and pH 7.4. When the release through F127 and T1107 gated hMSNs are compared the highest release rate is achieved with T1107 at 37℃ pH 4.8, and the lowest release rate is obtained with T1107 at 25℃ and pH 7.4.

In the second approach, functionalized surfaces of MSNs and modified copolymers are attached covalently by using click chemistry. For this purpose, aminated and carboxylated MSNs are produced and characterized first. Amination or carboxylation of MSNs are verified by FTIR spectroscopy analysis. With amine ended MSNs, an amine peak appears at 1540 cm^{-1} and a broad peak occurs from 2800 to 3300 cm^{-1} as a characteristic of N-H bending and stretching vibrations of primary amines. With carboxylated MSNs, carboxyl peaks are observed at 1650 cm^{-1} and 1410 cm^{-1}, Si-O-Si asymmetric stretching vibration are found at 1060cm^{-1}, and Si-OH asymmetric bending and stretching vibration are observed at 960 cm^{-1}. In addition, STEM analysis is performed to investigate the morphology and measure the average particle diameter of functionalized MSNs, which are ~230 nm for both aminated and carboxylated MSNs. Then, carboxylated/aminated T1107 and aminated F127 are produced by modifying the ends of the copolymers to enable the click chemistry. The functional groups are confirmed by FTIR. With carboxylated T1107, a peak associated with carbonyl stretching vibration appears at 1740 cm^{-1} indicating successful carboxylation. With amine-ended T1107 and F127, a peak for carbonyl group appears at 1720 cm^{-1}. With aminated T1107, two peaks (similar to camel hump shape) are also observed between 1500-1700 cm^{-1} indicating amide formation. After functionalization of copolymers, the gating is achieved by creating a chemical bond via EDAC between carboxylated MSN and aminated Pluronic/Tetronic, as well as aminated MSN and carboxylated Tetronic. The formation of the bond is verified via FTIR by observing two amide peaks between 1500 cm^{-1} -1700 cm^{-1} in the spectra, caused by NH2 and COOH reaction. Finally, cargo loading and release experiments are conducted. In this approach, arginine, which is hydrophilic, is selected as cargo molecule. Same temperature and pressure conditions are investigated; i.e. 25℃ and pH 7.4, 37℃ and pH 4.8, 37℃ and pH 7.4 as well as 43℃ and pH 7.4. With T1107 gated MSNs, the release of arginine is higher at low pH value (37℃ pH 4.8) as expected. With $MSNNH_2$-T1107COOH, the relase decreases in the following order: 43℃

and pH 7.4, 37℃ and pH 4.8, 37℃ and pH 7.4 and 25℃ and pH 7.4. Higher release rate at 43℃ and pH 7.4 is attributed to the break down of the gate due to the tempreture sensitive character of the material. With MSNCOOH-T1107NH_2, arginine release rate is the highest at 37℃ and pH 4.8, followed by those at 25℃ and pH 7.4, 43℃ and pH 7.4, 37℃ and pH 7.4. With MSNCOOH-F127NH_2, the release rate is higher at 25℃ and pH 7.4, followed by those at 37℃ and pH 7.4, 43℃ and pH 7.4, 37℃ and pH 4.8. The highest release rate is obtained with MSNCOOH-T1107NH_2. These findings suggest that MSNCOOH-F127NH_2 does not providean effective pH sensitive gating mechanism because it has the lowest release percentage at low pH. However, MSNCOOH-T1107NH_2 and MSNNH_2-T1107COOH are better options in terms of temperature sensitivity because they both have maximum release at low pH.

Finally, the cytotoxicity of synthesized nanoparticles is assessed at two different nanoparticle concentrations by using *S. cerevisiae* as a model cell and performing CFU analysis. The particles synthesized by physical approach are observed to be more toxic than those produced by chemical approach. Also, physical gating approach does not serve efficient drug release performance due to weak interactions between particle surface and copolymer. Therefore, in terms of drug release performance and toxicity, chemical attachment method is more preferable. Among the particles gated by chemical means, MSNCOOH-F127NH_2 and MSNNH_2-T1107COOH are observed to perform better than MSNCOOH-T1107NH_2 in terms of cell viability. Consequently, although MSNCOOH-T1107NH_2 is demonstrated to be more efficient in terms of gating mechanism, MSNNH_2-T1107COOH proves to be a better alternative considering the toxicity of the nanoparticles.

REFERENCES

1. Ferlay J., Soerjomataram I., Ervik M., Dikshit R., Eser S., Mathers C et al. GLOBOCAN 2012 v1.0, Cancer Incidence and Mortality Worldwide: IARC CancerBase No. 11 Lyon, France: International Agency for Research on Cancer; 2013.

2. Xu, X., Lü, S., Gao, C., Feng, C., Wu, C., Bai, X., . . . Liu, M. (2016). Self-fluorescent and stimuli-responsive mesoporous silica nanoparticles using a double-role curcumin gatekeeper for drug delivery. *Chemical Engineering Journal,300*, 185-192.

3. Vasir, J. K., & Labhasetwar, V. (2005). Targeted Drug Delivery in Cancer Therapy. *Technology in Cancer Research & Treatment*, 4(4), 363-374.

4. Xu, X., Lü, S., Gao, C., Wang, X., Bai, X., Duan, H., . . . Liu, M. (2015). Polymeric micelle-coated mesoporous silica nanoparticle for enhanced fluorescent imaging and pH-responsive drug delivery. *Chemical Engineering Journal*, 279, 851-860.

5. Yildirim, A., Demirel, G. B., Erdem, R., Senturk, B., Tekinay, T., & Bayindir, M. (2013). Pluronic polymer capped biocompatible mesoporous silica nanocarriers. *Chemical Communications*, 49(84), 9782.

6. Tang, F., Li, L., & Chen, D. (2012). ChemInform Abstract: Mesoporous Silica Nanoparticles: Synthesis, Biocompatibility and Drug Delivery. *ChemInform*, 43(20).

7. Ferenc, M., Katir, N., Milowska, K., Bousmina, M., Brahmi, Y., Felczak, A., . . . Kadib, A. E. (2016). Impact of mesoporous silica surface functionalization on human serum albumin interaction, cytotoxicity and antibacterial activity. Microporous and Mesoporous Materials, 231, 47-56.

8. Kabanov, A., Zhu, J., & Alakhov, V. (2005). Pluronic block copolymers for gene delivery. Advances in genetics, 53, 231-261.

9. Sharma, A. K., Zhang, L., Li, S., Kelly, D. L., Alakhov, V. Y., Batrakova, E. V., & Kabanov, A. V. (2008). Prevention of MDR development in leukemia cells by micelle-forming polymeric surfactant. Journal of Controlled Release, 131(3), 220-227.

10. Mogen, A. B., Chen, F., Ahn, S. J., Burne, R. A., Wang, D., & Rice, K. C. (2015). Pluronics-formulated farnesol promotes efficient killing and demonstrates novel interactions with Streptococcus mutans biofilms. PloS one, 10(7), e0133886.

11. Yasuda, S., Townsend, D., Michele, D. E., Favre, E. G., Day, S. M., & Metzger, J. M. (2005). Dystrophic heart failure blocked by membrane sealant poloxamer. Nature, 436(7053), 1025- 1029.

12. Cheng, C. Y., Wang, J. Y., Kausik, R., Lee, K. Y. C., & Han, S. (2012). Nature of interactions between PEO-PPO-PEO triblock copolymers and lipid membranes:(II) role of hydration dynamics revealed by dynamic nuclear polarization. Biomacromolecules, 13(9), 2624-2633.

13. Krylova, O. O., Melik-Nubarov, N. S., Badun, G. A., Ksenofontov, A. L., Menger, F. M., & Yaroslavov, A. A. (2003). Pluronic L61 accelerates flip–flop and transbilayer doxorubicin permeation. Chemistry-A European Journal, 9(16), 3930-3936.

14. Rahman, M., Yu, E., Forman, E., Roberson-Mailloux, C., Tung, J., Tringe, J., & Stroeve, P. (2014). Modified release from lipid bilayer coated mesoporous silica nanoparticles using PEO–PPO–PEO triblock copolymers. Colloids and Surfaces B: Biointerfaces, 122, 818-822.

15. Almeida, H., Amaral, M. H., & Lobao, P. (2012). Temperature and pH stimuli-responsive polymers and their applications in controlled and selfregulated drug delivery. Journal of Applied Pharmaceutical Science, 02(06), 01-10.

16. Ribeiro, A., Sosnik, A., Chiappetta, D. A., Veiga, F., Concheiro, A., & Alvarez-Lorenzo, C. (2012). Single and mixed poloxamine micelles as nanocarriers for solubilization and sustained release of ethoxzolamide for topical glaucoma therapy. Journal of The Royal Society Interface, 9(74), 2059-2069.

17. Slowing, I.I., Vivero-Escoto, J.L., Wu, C., & Lin, V.S. (2008). Mesoporous silica nanoparticles as controlled release drug delivery and gene transfection carriers. Advanced drug delivery reviews, 60 11, 1278-88.

18. Silveira, C. P., Apolinário, L. M., Fávaro, W. J., Paula, A. J., & Durán, N. (2015). Hybrid biomaterial based on porous silica nanoparticles and Pluronic F-127 for sustained release of sildenafil: In vivo study on prostate cancer. RSC Advances, 5(99), 81348-81355.

19. Yu, T., Malugin, A., & Ghandehari, H. (2011). Impact of Silica Nanoparticle Design on Cellular Toxicity and Hemolytic Activity. *ACS Nano,5*(7), 5717-5728.

20. Kim, I., Joachim, E., Choi, H., & Kim, K. (2015). Toxicity of silica nanoparticles depends on size, dose, and cell type. *Nanomedicine: Nanotechnology, Biology and Medicine,11*(6), 1407-1416.

21. Yildirim, A., & Bayindir, M. (2015). A porosity difference based selective dissolution strategy to prepare shape-tailored hollow mesoporous silica nanoparticles. J. Mater. Chem. A, 3(7), 3839-3846.

22. Tu, J., Boyle, A. L., Friedrich, H., Bomans, P. H., Bussmann, J., Sommerdijk, N. A., . . . Kros, A. (2016). Mesoporous Silica Nanoparticles with Large Pores for the Encapsulation and Release of Proteins. *ACS Applied Materials & Interfaces,8*(47), 32211-32219.

23. Yu, E., Lo, A., Jiang, L., Petkus, B., Ercan, N. I., & Stroeve, P. (2017). Improved controlled release of protein from expanded-pore mesoporous silica nanoparticles modified with co-functionalized poly(n-isopropylacrylamide) and poly(ethylene glycol) (PNIPAM-PEG). *Colloids and Surfaces B: Biointerfaces,149*, 297-300.

24. Coll, C., Mondragón, L., Martínez-Máñez, R., Sancenón, F., Marcos, M.D., Soto, J., Amorós, P. & Pérez-Payá, E., 2011. Enzyme-Mediated Controlled Release Systems by Anchoring Peptide Sequences on Mesoporous Silica Supports. Angewandte Chemie, 123(9), 2186-2188.

25. Kim, B. Y., Bae, J. W., & Park, K. D. (2013). Enzymatically in situ shell cross-linked micelles composed of 4-arm PPO–PEO and heparin for controlled dual drug delivery. Journal of Controlled Release,172(2), 535-540.

26. Seregina, M. V., Bronstein, L. M., Platonova, O. A., Chernyshov, D. M., Valetsky, P. M., Hartmann, J., . . . Antonietti, M. (1997). Preparation of Noble-Metal Colloids in Block Copolymer Micelles and Their Catalytic Properties in Hydrogenation. Chemistry of Materials, 9(4), 923-931.

27. Zhao, Y., Alakhova, D. Y., Kim, J. O., Bronich, T. K., & Kabanov, A. V. (2013). A simple way to enhance Doxil® therapy: Drug release from liposomes at the tumor site by amphiphilic block copolymer. Journal of Controlled Release, 168(1), 61-69.

28. Salmaso, S., & Caliceti, P. (2013). Stealth Properties to Improve Therapeutic Efficacy of Drug Nanocarriers. Journal of Drug Delivery, 2013, 1-19.

29. Hamidi, M., Azadi, A., & Rafiei, P. (2008). Hydrogel nanoparticles in drug delivery. Advanced Drug Delivery Reviews, 60(15), 1638-1649.

30. Hu, H., Lin, Z., He, B., Dai, W., Wang, X., Wang, J., . . . Zhang, Q. (2015). A novel localized co-delivery system with lapatinib microparticles and paclitaxel nanoparticles in a peritumorally injectable in situ hydrogel. Journal of Controlled Release, 220, 189-200.

31. Dehghankelishadi P., Dorkoosh FA. (2016). Pluronic based nano-delivery systems; Prospective warrior in war against cancer. Nanomed Res J, 1(1), 1-7.

32. Greenebaum, B., Blossfield, K., Hannig, J., Carrillo, C. S., Beckett, M. A., Weichselbaum, R. R., & Lee, R. C. (2004). Poloxamer 188 prevents acute necrosis of adult skeletal muscle cells following high-dose irradiation. Burns, 30(6), 539-547.

33. LS Instruments AG. (n.d.), *Dynamic Light Scattering*, https://lsinstruments.ch/en/technology/dynamic-light-scattering-dls, accessed in June 2019

34. Ojeda, J. J., & Dittrich, M. (2012). Fourier Transform Infrared Spectroscopy for Molecular Analysis of Microbial Cells. *Microbial Systems Biology Methods in Molecular Biology*,187-211.

35. Applications of Nanotechnology. (2016). *Essentials in Nanoscience and Nanotechnology*,361-418.

36. Home. (2019, May 09), *Seeing the Light: An Overview of Visible and UV-VIS Spectroscopy*, https://www.coleparmer.com/tech-article/visible-and-uv-vis-spectroscopy, accessed in July 2019

37. Stober, W.; Fink, A.; Bohn, E. Controlled growth of monodisperse silica spheres in the micron size range. J. Colloid Interface Sci. 1968, 26, 62–69.

38. Han, C., Huang, H., Dong, Y., Sui, X., Jian, B., & Zhu, W. (2019). A Comparative Study of the Use of Mesoporous Carbon and Mesoporous Silica as Drug Carriers for Oral Delivery of the Water-Insoluble Drug Carvedilol. *Molecules,24*(9), 1770.

39. Zhang, W., Shi, Y., Chen, Y., Ye, J., Sha, X., & Fang, X. (2011). Multifunctional Pluronic P123/F127 mixed polymeric micelles loaded with paclitaxel for the treatment of multidrug resistant tumors. *Biomaterials,32*(11), 2894-2906.

40. Park, K. M., Shin, Y. M., Joung, Y. K., Shin, H., & Park, K. D. (2010). In Situ Forming Hydrogels Based on Tyramine Conjugated 4-Arm-PPO-PEO via Enzymatic Oxidative Reaction. *Biomacromolecules,11*(3), 706-712.

41. Bhattacharyya, S., Wang, H., & Ducheyne, P. (2012). Polymer-coated mesoporous silica nanoparticles for the controlled release of macromolecules. *Acta Biomaterialia,8*(9), 3429-3435.

42. Tannock, I. F.; Rotin, D. Acid pH in tumors and its potential for therapeutic exploitation. Cancer Res., 1989, 49, 4373-4384.

43. Lisi, R. D., Giammona, G., Lazzara, G., & Milioto, S. (2011). Copolymers sensitive to temperature and pH in water and in water oil mixtures: A DSC, ITC and volumetric study. *Journal of Colloid and Interface Science,354*(2), 749-757.

44. Kim, T., Kim, M., Eltohamy, M., Yun, Y., Jang, J., & Kim, H. (2012). Efficacy of mesoporous silica nanoparticles in delivering BMP-2 plasmid DNA forin vitroosteogenic stimulation of mesenchymal stem cells. *Journal of Biomedical Materials Research Part A,101A*(6), 1651-1660.

45. Suteewong, T., Sai, H., Bradbury, M., Estroff, L. A., Gruner, S. M., & Wiesner, U. (2012). Synthesis and Formation Mechanism of Aminated Mesoporous Silica Nanoparticles. *Chemistry of Materials,24*(20), 3895-3905.

46. Feifel, S. C., & Lisdat, F. (2011). Silica nanoparticles for the layer-by-layer assembly of fully electro-active cytochrome c multilayers. *Journal of Nanobiotechnology*,*9*(1), 59.

47. Basak, R., & Bandyopadhyay, R. (2013). Encapsulation of Hydrophobic Drugs in Pluronic F127 Micelles: Effects of Drug Hydrophobicity, Solution Temperature, and pH. Langmuir, 29(13), 4350-4356.

48. Gentile, L., Antunes, F. E., Luca, G. D., & Oliviero, C. (2010). Thermogelation Analysis Of F127-Water Mixtures By Physical Chemistry Techniques. *Applied Rheology*,*20*(5).

49. Khan, I., Saeed, K., & Khan, I. (2017). Nanoparticles: Properties, applications and toxicities. *Arabian Journal of Chemistry*.

50. Alvarez-Lorenzo, C., Rey-Rico, A., Sosnik, A., & Taboada, P. (2010). Poloxamine-based nanomaterials for drug delivery. *Frontiers in Bioscience*, E2(2), 424-440.

51. Wang, L., Wu, L., Lu, S., Chang, L., Teng, I., Yang, C., & Ho, J. A. (2010). Biofunctionalized Phospholipid-Capped Mesoporous Silica Nanoshuttles for Targeted Drug Delivery: Improved Water Suspensibility and Decreased Nonspecific Protein Binding. ACS Nano, 4(8), 4371-4379.

52. Chang, D., Gao, Y., Wang, L., Liu, G., Chen, Y., Wang, T., . . . Zeng, X. (2015). Polydopamine-based surface modification of mesoporous silica nanoparticles as pH-sensitive drug delivery vehicles for cancer therapy. Journal of Colloid and Interface Science, 463, 279-287.

53. Kaur, S., Prasad, C., Balakrishnan, B., & Banerjee, R. (2015). Trigger responsive polymeric nanocarriers for cancer therapy. Biomater. Sci., 3(7), 955-987.

54. Song, X., Chen, Q., & Liu, Z. (2014). Recent advances in the development of organic photothermal nano-agents. Nano Research, 8(2), 340-354.

55. Bakshi, M. S. (2014). Colloidal micelles of block copolymers as nanoreactors, templates for gold nanoparticles, and vehicles for biomedical applications. Advances in Colloid and Interface Science, 213, 1-20.

56. Liu, L., Yong, K., Roy, I., Law, W., Ye, L., Liu, J., . . . Prasad, P. N. (2012). Bioconjugated Pluronic Triblock-Copolymer Micelle-Encapsulated Quantum Dots for Targeted Imaging of Cancer: In Vitro and In Vivo Studies. *Theranostics,2*(7), 705-713.

57. Zalipsky, S., Gilon, C., & Zilkha, A. (1983). Attachment of drugs to polyethylene glycols. *European Polymer Journal,19*(12), 1177-1183.

58. Singh, V., Khullar, P., Dave, P. N., & Kaur, N. (2013). Micelles, mixed micelles, and applications of polyoxypropylene (PPO)-polyoxyethylene (PEO)-polyoxypropylene (PPO) triblock polymers. International Journal of Industrial Chemistry, 4(1), 12.

59. Mishra, S., Peddada, L. Y., Devore, D. I., & Roth, C. M. (2012). Poly(alkylene oxide) Copolymers for Nucleic Acid Delivery. Accounts of Chemical Research, 45(7), 1057-1066.

APPENDIX A: RESULTS OF DLS AND ZETA POTENTIAL ANALYSES

Sample ID	T1107 (Combined)
Operator ID	BBGU
Elapsed Time	00:08:00
Mean Diam.	306.0 nm
Rel. Var.	0.180
Skew	4.702

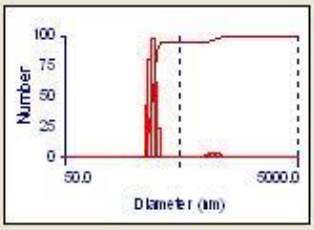

d(nm)	G(d)	C(d)	d(nm)	G(d)	C(d)	d(nm)	G(d)	C(d)
199.0	0	0	378.6	0	96	720.0	0	96
211.0	0	0	401.3	0	96	763.4	0	96
223.7	0	0	425.5	0	96	809.3	1	96
237.2	0	0	451.1	0	96	858.0	2	97
251.4	42	13	478.3	0	96	909.7	3	98
266.6	82	38	507.1	0	96	964.5	3	99
282.6	100	69	537.6	0	96	1022.5	3	100
299.6	63	89	569.9	0	96	1084.0	1	100
317.7	23	96	604.2	0	96	1149.3	0	100
336.8	0	96	640.6	0	96	1218.5	0	100
357.1	0	96	679.2	0	96	1291.8	0	100

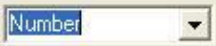

Figure A.1. DLS Results of T1107 coated hMSNs

Sample ID	F127 (Combined)
Operator ID	BBGU
Elapsed Time	00:07:00
Mean Diam.	718.3 nm
Rel. Var.	0.000
Skew	-0.003

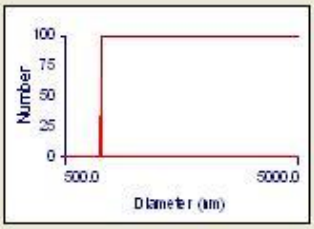

d(nm)	G(d)	C(d)	d(nm)	G(d)	C(d)	d(nm)	G(d)	C(d)
694.5	0	0	712.9	15	4	727.4	0	100
696.0	0	0	714.2	33	10	730.2	0	100
697.5	0	0	715.5	61	22	731.8	0	100
699.0	0	0	716.8	88	39	733.4	0	100
700.6	0	0	718.1	100	58	735.0	0	100
702.1	0	0	719.5	91	75	736.6	0	100
703.6	0	0	720.8	67	88	738.2	0	100
705.2	0	0	722.1	39	95	739.8	0	100
706.7	0	0	723.4	18	99	741.5	0	100
708.2	0	0	724.7	7	100	743.1	0	100
711.6	5	1	726.1	0	100	744.7	0	100

Figure A.2. DLS Results of F127 coated hMSNs

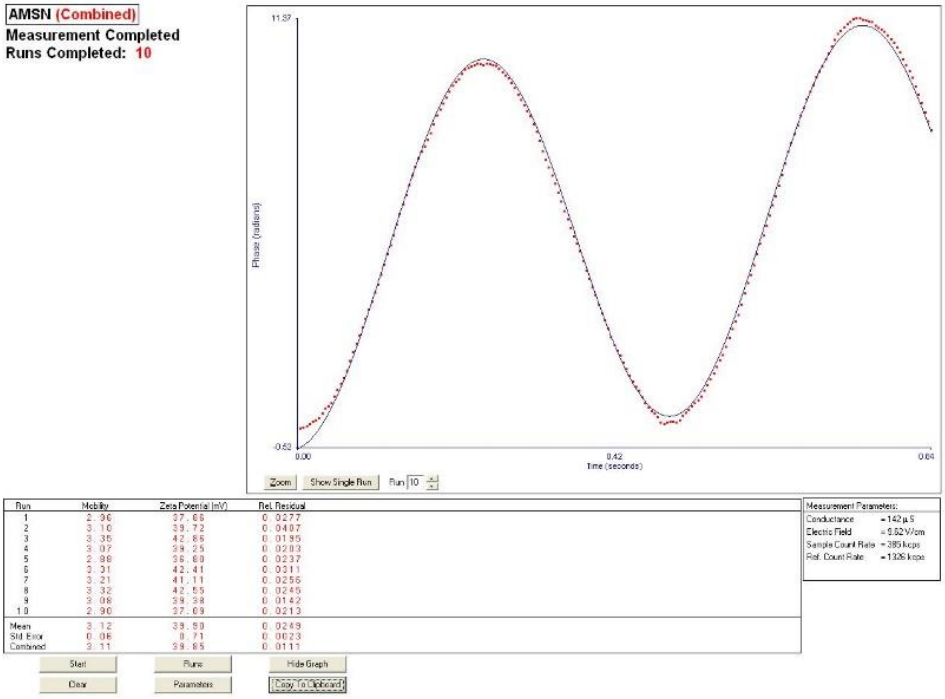

Figure A.3. Zeta Potential Results of $MSNNH_2$

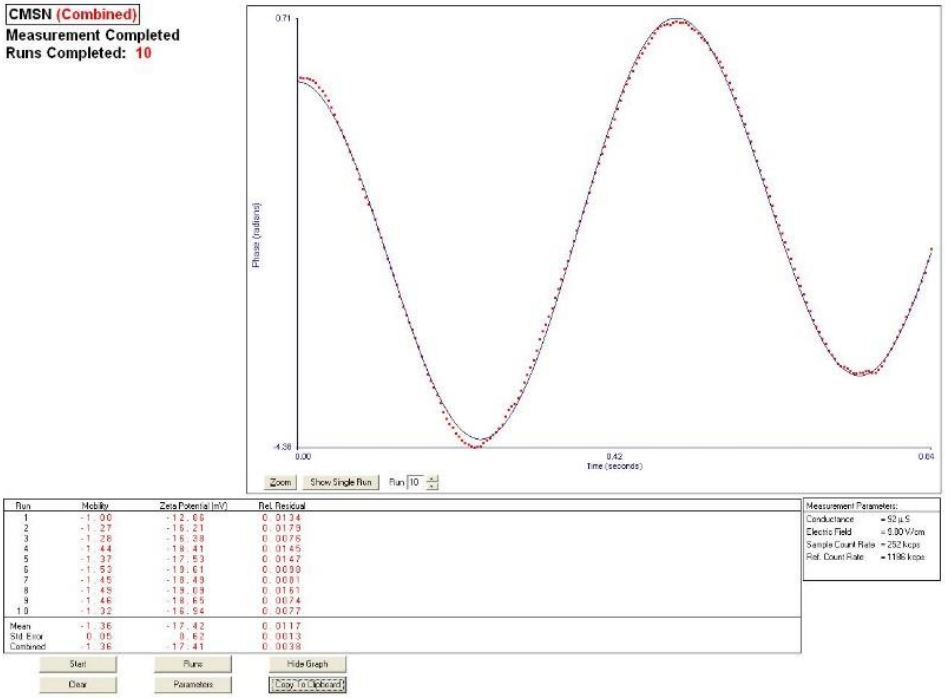

Figure A.4. Zeta Potential Results of MSNCOOH

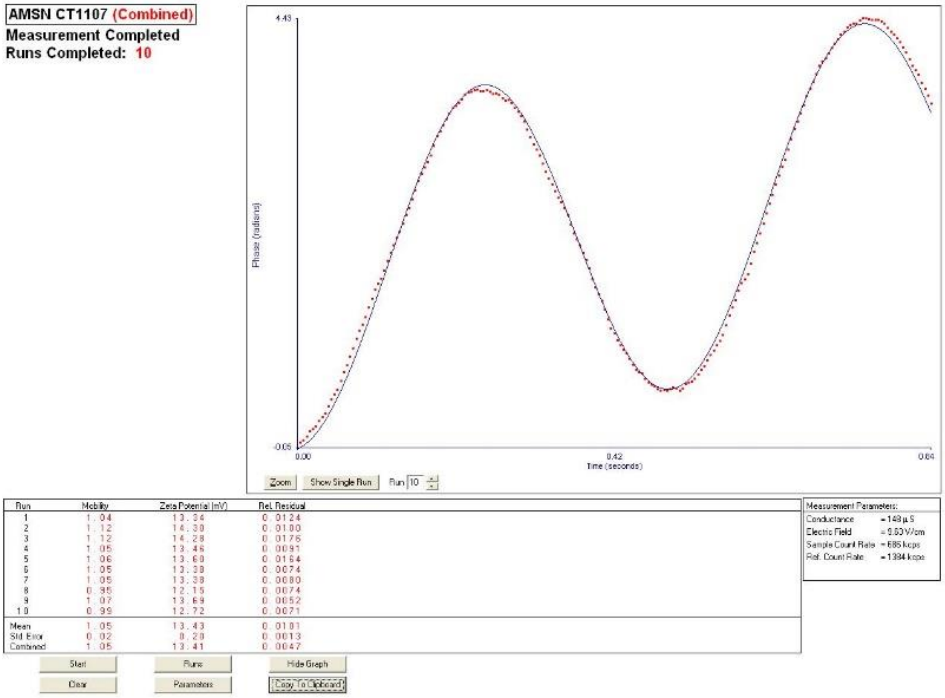

Figure A.5. Zeta Potential Results of MSNNH$_2$-T1107COOH

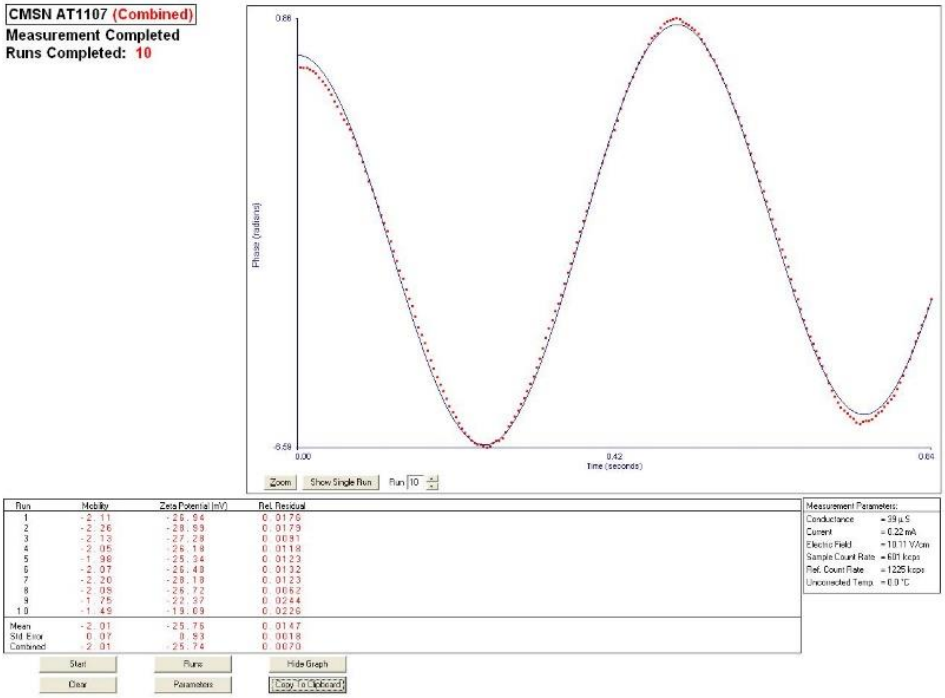

Figure A.6. Zeta Potential Results of MSNCOOH-T1107NH$_2$

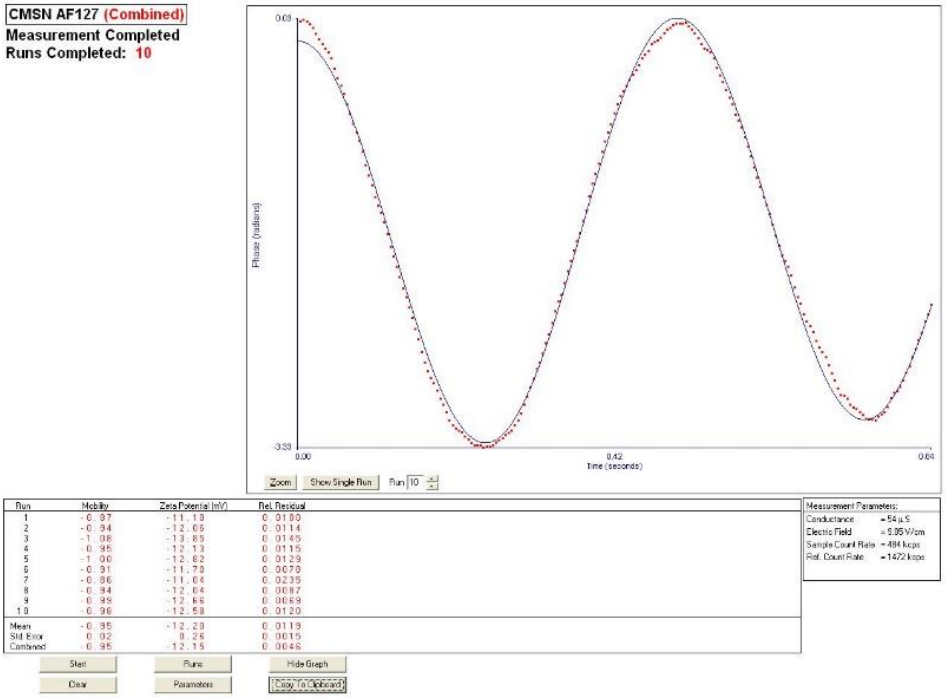

Figure A.7. Zeta Potential Results of MSNCOOH-F127NH_2